Relocation of inactive X chromatin during S phase: the role of CIZ1

Robert Matthew Lewis Turner (BSc)

MSc (by research)

University of York
Biology

December 2018

Abstract

X chromosome inactivation (XCI) allows the establishment of gene dosage compensation between male and female mammals. The long non-coding RNA *Xist* recruits polycomb repressive complexes (PRC), forming transcriptionally silent heterochromatin, involving accumulation of H2AK119Ub1 and H3K27me3. The nuclear matrix protein CIZ1 is required for retention of *Xist* and co-localizes with enriched H3K27me3 marks at the inactive X chromosome (Xi), allowing Xi to be used as a model to study CIZ1.

Data presented here confirms dynamic localization of the Xi towards a perinucleolar zone, followed by relocation back to the nuclear periphery after its replication. Genetic deletion of CIZ1 resulted in loss of internalization, suggesting that CIZ1 plays a crucial role in Xi relocation, which is the first documented protein required for Xi movement. Culture adaptation also resulted in loss of internalization, suggesting the relocation mechanism is prone to degeneration. Results suggest that CIZ1 is required for PRC function at the Xi, evidenced by loss of H2AK119Ub1 and H3K27me3 in CIZ1 null cells. Unexpectedly, re-emergence of chromatin modifications occurred upon culture adaptation of CIZ1 null cells. Alongside recent observations of a shift in isoform of PRC2 catalytic subunit EZH2 and increase in protein level and solubility, the data presented here suggest that primary cells and culture adapted cells use different pathways to ensure that Xi chromatin and modifying enzymes meet. This analysis reinforces the hypothesis that cell lines do not represent the physiological functional state of cells, having implications for future research in cancer biology.

EdU incorporation and thymidine arrest, the new alternative assay developed here, have allowed for the first time the requirements of Xi relocation to be explored. Preliminary data suggests that Xi departure occurs via a pathway involving nuclear myosin, requiring DNA polymerase α function, while Xi return occurs via (nuclear or cytoplasmic) dynein and nuclear myosin-based pathways.

Table of Contents

List of Figures

List of Tables

Acknowledgements

I would like to thank my supervisor Prof. Dawn Coverley for her nonstop support and excellent advice, without which I would not have developed into the scientist I am today. I would also like to thank Dr. Justin Ainscough for his support and technical guidance, and Emma Stewart for intellectual conversation and development of ideas within the Coverley lab. Thanks also go to others at York that have made my time this year so memorable, specifically Matthew Warren for easy FIFA wins, and all members of UYRUFC for much needed release from lab work.

I would also like to thank Victoria Scott for generating EdU incorporation data on E13.1 p25 and E14.4 p10, and Justin Ainscough for providing all cells and cell lines used in this study.

Finally, I would like to thank my parents for their encouragement, unconditional care since day one and for making all this possible, my sister Sarah for weekly shopping trips and lunches, and my lovely girlfriend Grace for constantly putting a smile on my face and for making each day more bearable.

I have thoroughly enjoyed my time in the Coverley lab and I am eternally grateful for the opportunity and experience.

Author's Declaration

I declare that this thesis is a presentation of original work and I am the sole author. This work has not previously been presented for an award at this, or any other, University. All sources are acknowledged as References.

All research in this thesis is my own, with the following exceptions:

All primary embryonic fibroblasts (wild type and CIZ1 null) were generated by Justin Ainscough.

Chapter 3:

Western blot (Figure 3.3.A) was reproduced from Turner 2017.

Chapter 4:

Data for wild type E13.1 p25 EdU pulse and chase (Figure 4.4A) was generated by Victoria Scott.

Chapter 5 and 6:

Aphidicolin used to test requirement of ongoing DNA synthesis was kindly provided by Emma Stewart.

Appendices:

Appendix A and D were taken from Stewart et al. 2018.
Data for wild type E14.4 p10 EdU pulse and chase (Appendix C) was generated by Victoria Scott.

Work in press

The work presented in the following chapters has been accepted for publishing as part of a journal article entitled:

Stewart, E., Turner, R., et al. (2018). Maintenance of epigenetic landscape requires CIZ1 and is corrupted in differentiated fibroblasts in long-term culture. To be published in Nat. Commun. [Paper #NCOMMS-18-15349B].

- Chapter 3. The role of CIZ1 in Polycomb complex function at the Xi.
- Chapter 4. Exploiting the EdU (5-ethynyl-2'-deoxyuridine) assay to study the location of the inactive X chromosome during S phase.

Chapter 1. Introduction

1.1 X chromosome inactivation

X chromosome inactivation (XCI) is a mechanism that allows the establishment of gene dosage compensation between male and female mammals (Gribnau and Grootegoed 2012). This process prevents double dosage of genes located on the X chromosome in females (Lyon 1961), female cells having two X chromosomes (XX) and male cells only having one (XY). One of the two X chromosomes in female cells is inactivated, subsequently condensing into a Barr body (Barr and Bertram 1949), whilst the other X chromosome remains transcriptionally active. Key to the process of XCI is *Xist* (X inactive specific transcript). *Xist* is a 17kb long non-coding RNA (lncRNA) molecule that is expressed from the X chromosome inactivation centre (XIC), the regulatory locus on the X chromosome (Galupa and Heard 2015). Xist has been shown to consist of several conserved repeat domains, labelled A to F, which have separate roles in XCI (Brown et al. 1992; Sado and Brockdorff 2013). Repeat A is required for transcript silencing while repeats B, E and F play a role in the recruitment of complexes that result in silencing (da Rocha et al. 2014) and repeat C facilitates the association of *Xist* RNA to the X chromosome (Sado and Brockdorff 2013). RNA sequencing in mice has shown that *Xist* plays a vital role in dosage compensation and that *Xist* is needed to avoid failure of the process as early as the blastocyst stage (Borensztein et al. 2017).

Differentiation is accompanied by the initiation of random XCI. Initiation occurs via stimulation of the downregulation of pluripotency factors, such as Oct4 and Klf4, which bind and repress *Xist* expression and upregulate *Tsix* expression (Navarro et al. 2008). *Tsix* is a non-coding gene antisense to *Xist* that suppresses *Xist* transcription (Lee et al. 1999). As well as this, *Xist* activators, such as *Rnf12,* and a cis-regulatory region containing Jpx, Ftx, and Xpr are upregulated (Jonkers et al. 2009; Barakat et al. 2014). Jpx, Ftx and Xpr act together to allow *Rnf12* to activate *Xist.* Together these result in the upregulation of *Xist* at the chromosome that has been chosen to become the inactive X

chromosome (Xi) (Augui et al. 2011). Following this, *Xist* transcripts spread *in cis*- along the X chromosome (Figure 1.1), accumulating and forming a coat which leads to the formation of transcriptionally silent heterochromatin via the regulation of gene expression by polycomb group protein action (Muyrers-Chen et al. 2004; Wiles and Selker 2017).

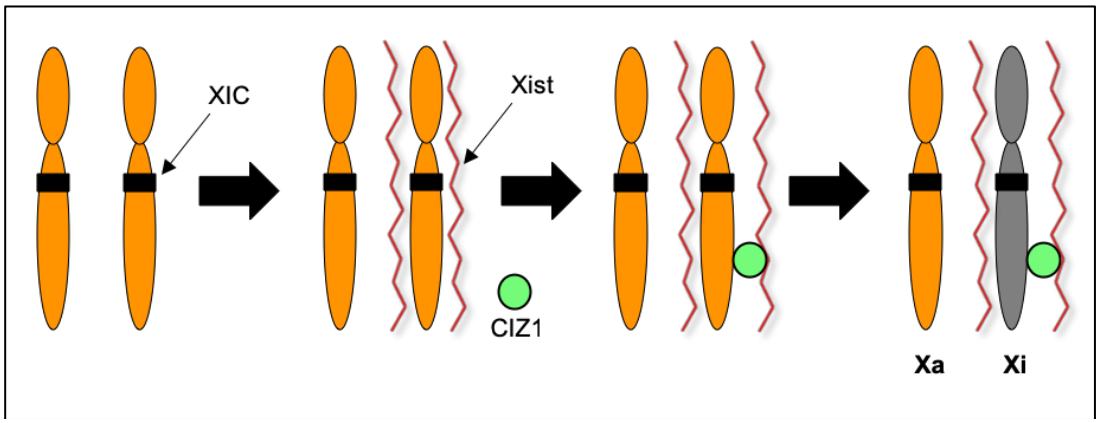

Figure 1.1. Schematic showing the process of X chromosome inactivation.
X chromosome inactivation is initiated by expression of Xist from the X chromosome inactivation centre (XIC) of the X chromosome destined to become inactivated. CIZ1 (CIP/CDKN1A-interacting zinc finger protein 1) is recruited to the Xi by Xist repeat E, subsequently anchoring Xist to the Xi. "Xa" indicates the active X chromosome, "Xi" indicates the transcriptionally silent and inactive X chromosome.

Polycomb group proteins (PcGs) are epigenetic transcriptional repressors and regulators of cell fate in mammals (Schwartz and Pirrotta 2007) and can be divided into two chromatin-associated complexes: Polycomb Repressive Complex 1 (PRC1) and Polycomb Repressive Complex 2 (PRC2). Both PRC1 and PRC2 are composed of several subunits and are responsible for different chromatin modifications at the Xi (Figure 1.2). The core of PRC1 includes a single variant of each of the subunits PCGF (Polycomb group ring finger), CBX (chromobox-containing protein), PHC (polyhomeotic subunit) and RING1A/B (ring finger protein) (Levine et al. 2002; Valk-Lingbeek et al. 2004). RING1 protein activation results in monoubiquitylation E3 ligase activity that is specific for lysine 119 on histone 2A (H2AK119Ub), causing repression of chromatin (Wang et al. 2004; de Napoles et al. 2004). PRC2 is the less complex of the two, with the core including SUZ12 (suppressor of zeste 12 homolog), EED (embryonic ectoderm

development), RBAP (histone binding protein) and either EZH1 or EZH2 (enhancer of zeste) subunits (Cao et al. 2002; Kuzmichev et al. 2002). EZH1 or EZH2 activation results in trimethylation of lysine 27 on histone 3 (H3K27me3), leading to the production of transcriptionally silent heterochromatin via regulation of gene expression (Margueron and Reinberg 2011; Wiles and Selker 2017). It has been shown that PRC1 initiates PRC recruitment via the interaction of the RNA-binding protein hnRNPK and sequences encoded by *Xist* repeat B (Pintacuda et al. 2017). PRC2 has also been shown to be recruited by *Xist* during the early stages of XCI, with the RNA-binding protein ATRX aiding in attachment of the two (Sarma et al. 2014). In addition, PRC2 associates with the zinc finger protein AEBP2 and the Jumonji protein JARID2 (Kim et al. 2009; da Rocha et al. 2014), both of which play a role in targeting and recruitment of PRC2 to the X chromosome (Schwartz and Pirrotta 2013). The polycomb cascade results in the accumulation of H2AK119Ub (PRC1) and H3K27me3 (PRC2) on the Xi, which is maintained during progression through rounds of cell division (Almeida et al. 2017).

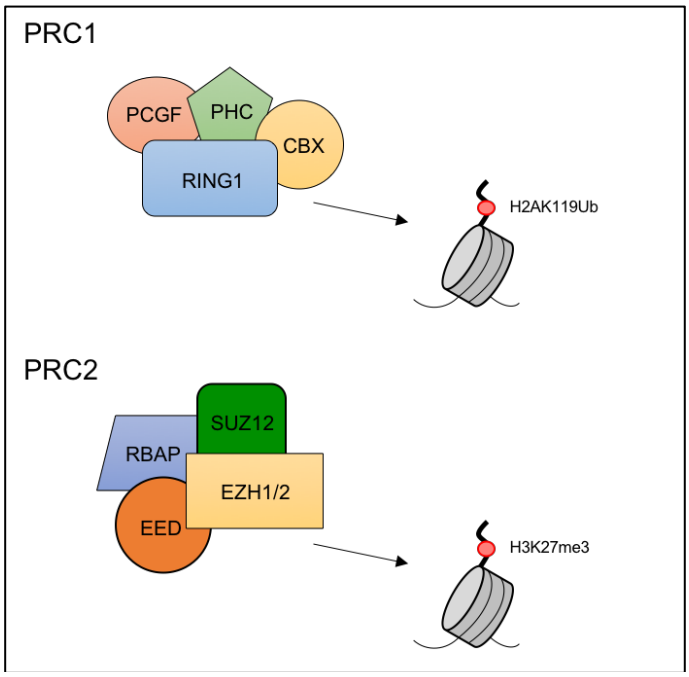

Figure 1.2. Schematic showing the composition and function of PRC1 and PRC2. Canonical PRC1 contains subunits of PCGF (Polycomb group ring finger), CBX (chromobox-containing protein), PHC (polyhomeotic subunit) and RING1A/B (ring finger protein), which results in monoubiquitylation of histone H2A at lysine 119. Canonical PRC2 contains subunits of SUZ12 (suppressor of zeste 12 homolog), EED (embryonic ectoderm development), RBAP (histone binding protein) and EZH1/2 (enhancer of zeste), which results in trimethylation of histone H3 at lysine 27.

1.2 The nuclear matrix

Interestingly, *Xist* is able to avoid nuclear export, remaining in the nucleus, in order to coat the Xi. The nuclear matrix protein SAF-A (scaffold attachment factor A), also known as hnRNPU (heterogeneous nuclear ribonucleoprotein U) has been suggested to play a role in the localisation of *Xist* RNA to the Xi, with knockdown of SAF-A resulting in lack of localization and loss of H3K27me3 (Hasegawa et al. 2010). The term nuclear matrix was first used to describe the network of residual fibres that was left within the nucleus when lipids, soluble proteins, chromatin and in some cases RNA are removed (Berezney and Coffey 1974). The nuclear matrix has been suggested to have a role in multiple cellular processes such as DNA transcription (Robinson et al. 1983), DNA repair (Koehler and Hanawalt 1996), DNA replication (Anachkova et al. 2005) and pre-

mRNA splicing (Zeitlin et al. 1987), although its exact function and composition is still unknown and thought to vary between cell types. Recently, CIP/CDKN1A-interacting zinc finger protein 1 (CIZ1) has been found to be associated with the RNA fraction of the nuclear matrix dependent on *Xist* repeat E (Ridings-Figueroa et al. 2017), possibly via direct interaction.

1.3 CIP/CDKN1A-interacting zinc finger protein 1

CIP/CDKN1A-interacting zinc finger protein 1 (CIZ1) has been identified as a nuclear matrix protein that is encoded by 17 exons. These 17 exons are alternatively spliced with currently over 22 known variants (Rahman et al. 2010). CIZ1 was first identified via its ability to bind to the cyclin-dependent kinase inhibitor p21, which causes cell cycle arrest via inhibition of DNA replication (Mitsui et al. 1999). Furthermore, CIZ1 has been found to play an important role in the promotion of mammalian DNA replication (Coverley et al. 2005). More recently, CIZ1 has been reported to interact with cyclin-dependent kinase 2 (CDK2), cyclin E, cyclin A via RXL cycling binding motifs, and the pre-replication factor CDC6 (Copeland et al. 2010; Copeland et al. 2015). During mid-G1 phase of the cell cycle, cyclin E interacts with CDK2 in order to allow the assembly of the pre-replication complex. For progression through S phase to occur, levels of cyclin A rise, causing cyclin A to displace cyclin E as the molecular partner of CDK2. This ultimately leads to activation of the DNA replication machinery and subsequently cell cycle progression. CIZ1 consists of two characterised domains (Coverley et al. 2005); an N-terminal domain and a C-terminal domain (Figure 1.3). *In vitro*, the relative affinities of cyclin E and A for sites in the N-terminal domain of CIZ1 suggest sequential interaction (Copeland et al. 2010). The C-terminal domain tethers CIZ1 to the nuclear matrix, in a cell cycle dependent manner, possibly enabling its observed co-localization with DNA replication factories (Ainscough et al. 2007). Moreover, the C-terminal nuclear matrix interaction domain is capable of incorporation into the nuclear matrix if the N-terminal domain is absent (Ainscough et al. 2007). These characterised domains have been suggested to allow CIZ1 to control DNA replication in a spatial and temporal manner, specifying the location in the nucleus at which cyclin exchange occurs, as well as acting as a scaffold for the delivery of cyclins to replication factories.

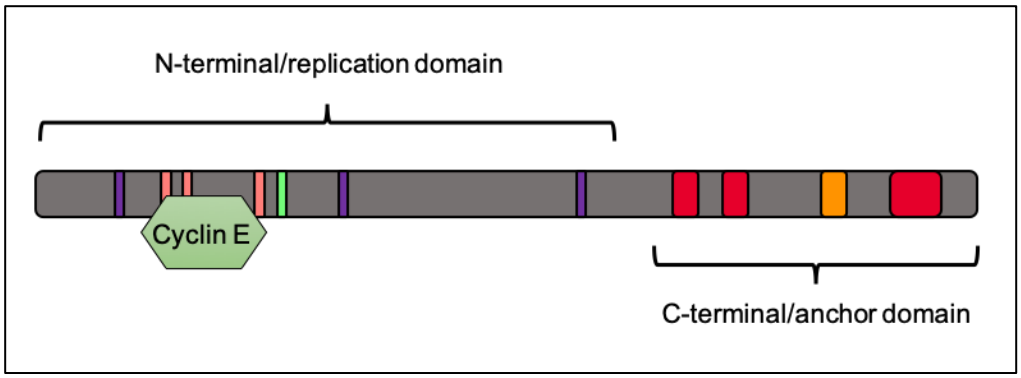

Figure 1.3. Schematic showing characterised domains of CIZ1 protein.
The N-terminal domain acts as a scaffold for cyclin exchange, resulting in DNA replication, containing the nuclear localisation signal (green), the functional CDK phosphorylation sites (pink) and the RXL cyclin-binding motifs (purple). The C-terminal domain tethers CIZ1 to the nuclear matrix, containing C2H2-type zinc fingers and matrin3-type RNA binding zinc finger (red) and an acidic domain (orange).

As mentioned above, CIZ1 is recruited to the Xi by sequences encoded by *Xist* repeat E during early stages of XCI (Ridings-Figueroa et al. 2017; Sunwoo et al. 2017; Figure 1.1). Interestingly, because XCI is known to be essential for embryonic development, the implication is that CIZ1 is not required during the early stages. This is because CIZ1 null mice display no overt embryonic phenotype (Ridings-Figueroa et al. 2017). Conversely, CIZ1 is required for retention of Xist at the Xi in differentiated cells, as shown via delocalisation of Xist and loss of H3K27me3 in fibroblasts from CIZ1 null mice (Ridings-Figueroa et al. 2017). This implies a role in the maintenance of XCI, rather than its initiation. High intensity patches of CIZ1 can be detected at the Xi in differentiated somatic cells, using the anti-CIZ1 antibody 1794 (Coverley et al. 2005), and have been shown to co-localize with enriched marks of H3K27me3 (Ridings-Figueroa et al. 2017), which are characteristic of XCI. Therefore, it is possible to utilize the Xi as a well-defined model in order to uncover the mechanism of action and function of CIZ1.

1.4 Culture adaptation of cells

Normal cells possess a limited capability to divide. Once this limit is reached, the cells cease to grown and subsequently enter replicative senescence or crisis (Hayflick and Moorhead 1961), a separate stage outside of the regular cell cycle. This withdrawal from the cell cycle is triggered as a consequence of the shortening of telomeres (Lundblad and Szostak 1989; Bodnar et al. 1998), protective nucleoprotein structures found at the ends of chromosomes. Normally, DNA replication machinery is unable to complete replication of chromosomal ends (Watson 1972), resulting in loss of sequence with each round of cellular division, leading to senescence and ultimately cell death (Harley et al. 1990). Culture adaptation occurs when a subpopulation of cells acquires an advantage via a mutation in the promoter of the telomerase gene causing upregulation of telomerase, a ribonucleoprotein responsible for adding a repeat sequence to the end of telomeres. This allows the subpopulation to escape senescence and continue to divide (Shay et al. 1991). Culture adapted cells are invaluable tools in cell biology, being able to be grown indefinitely *in vitro*, however they may also have sustained many other uncharacterised changes.

1.5 Chromosomal movement

The Xi is normally located at the nuclear periphery, anchored via the lamin B receptor (Chen et al. 2016), and is believed to replicate in late S phase. Even the earliest studies on Xi location have suggested that the Xi is able to occupy a second distinct region towards the interior of the nucleus (Barr and Bertram 1949). After XCI, beyond embryonic days 5.5, the Xi is said to enter a maintenance phase allowing propagation of the transcriptionally silent state through cell division (Yildirim et al. 2013). During S phase, it has been suggested that the Xi migrates to the perinucleolar zone in a transient manner to allow maintenance of epigenetic modifications (Zhang et al. 2007). Interestingly, *Xist* was found to play a key role in the targeting of the Xi to the perinucleolar zone, loss of *Xist* results in the loss of internalisation and loss of H3K27me3, leading to reactivation of some genes on the Xi. *Xist* is not the only lncRNA that has been suggested to be involved in long-range chromosomal movement. The lncRNA *Firre* has been shown to anchor the Xi towards the nucleolus, allowing

maintenance of H3K27me3 (Yang et al. 2015). Furthermore, in an example unrelated to the Xi, the non-coding RNA Kcnq1ot1 has been implicated in mediating silencing of linked genes via H3K27me3 via perinucleolar targeting of an episomal vector during S phase (Pandey et al. 2008; Mohammad et al. 2008). Therefore existing evidence is suggesting that lncRNAs play a role in chromatin relocation, often leading to maintenance of epigenetic transcriptional silencing.

Long-range chromatin movement has previously been studied using tagged loci and live cell imaging approaches in Chinese hamster ovary (CHO) cells, reporting inducible unidirectional migration of an engineered locus from the nuclear periphery to the interior (Chuang et al. 2006). Another example of chromatin movement is evident during progression through the G0 (quiescence) and G1 transition, with the Xi moving from the periphery to the nucleolus (Lyu et al. 2018). Chromatin movement has also been studied in transformed cells, where distinct nuclear positions were identified, although no evidence for transient relocation was reported (Chubb et al. 2002). There is currently no universally accepted mechanism for chromosome movement.

1.6 Relevance in a clinical setting

CIZ1 has been linked with an ever-growing list of devastating diseases and disorders. These include neurological disorders cervical dystonia (Xiao et al. 2012) and Alzheimer's disease (Dahmcke et al. 2008), as well as a range of cancers, including paediatric cancers such as Ewing sarcoma (Rahman et al. 2007) and adult cancers such as breast cancer (den Hollander et al. 2006), lung cancer (Higgins et al. 2012), colon cancer (Wang et al. 2014), gallbladder cancer (Zhang et al. 2015), prostate carcinoma (Liu et al. 2015) and gastric cancer (Kim et al. 2004). Moreover, CIZ1 has recently been linked with promoting tumour growth and metastasis in hepatocellular carcinoma (Wu et al. 2016). As mentioned, CIZ1 plays a crucial role in cell cycle progression, therefore it has been suggested that altered CIZ1 is part of tumour formation instead of a consequence. PRC1/2 have also been linked with cancer, having roles in pathways that are routinely disrupted in cancer (Baylin and Jones 2011). Furthermore, overexpression of PRCs has been seen in several cancers, such as lymphoma (Raaphorst 2005), lung cancer (Sato et al. 2013) and breast cancer

(Yoo and Hennighausen 2012). In addition, XCI has been linked with cancer following the finding that the Xi is lost in breast cancer cells (Sirchia et al. 2005). Interestingly, genetic deletion of CIZ1 led to 100% of female mice developing non-Hodgkin follicular lymphoma (Ridings-Figueroa et al. 2017). Although not well understood mechanistically, this suggests that CIZ1 may have a role as a tumour suppressor as well as a tumour promoter.

Cancer, disease or disorder	Reference
Cervical dystonia	(Xiao et al. 2012)
Alzheimer's disease	(Dahmcke et al. 2008)
Ewing sarcoma	(Rahman et al. 2007)
Breast cancer	(Sirchia et al. 2005); den Hollander et al. 2006; Yoo and Hennighausen 2012)
Lung cancer	(Higgins et al. 2012; Sato et al. 2013)
Colon cancer	(Wang et al. 2014)
Gallbladder cancer	(Zhang et al. 2015)
Prostate carcinoma	(Liu et al. 2015)
Gastric cancer	(Kim et al. 2004)
Hepatocellular carcinoma	(Wu et al. 2016)
Lymphoma	(Raaphorst 2005)
Non-Hodgkin follicular lymphoma	(Ridings-Figueroa et al. 2017)

Table 1. Cancers, diseases and disorders associated with CIZ1, PRC1/2 and XCI.

Altogether, these observations highlight the clinical relevance and importance of studies that look to aid in developing understanding of the normal biological function of proteins, such as CIZ1, that are apparent to have a significant contribution to cancer biology.

1.7 Project aims

The aims of this project are as follows:

- To investigate the role CIZ1 and culture adaptation play in PRC function. (Chapter 3)
- To investigate the relationship between CIZ1 and the dynamic relocation of chromatin during S phase, and explore the effect of culture adaptation. (Chapter 4)
- To take the first steps towards characterisation of the requirements for CIZ1-dependent chromosomal movement within the nucleus. (Chapter 5 and 6)

Chapter 2. Materials and Methods

2.1 Cell Culture

2.1.1 Cell Line Information

Cell Line	Type	♀/♂	Genotype
E13.1	Primary embryonic fibroblast	♀	Wild-type
E13.8	Primary embryonic fibroblast	♀	Wild-type
E14.4	Primary embryonic fibroblast	♀	Wild-type
E13.15	Primary embryonic fibroblast	♀	CIZ1 Null
E13.17	Primary embryonic fibroblast	♀	CIZ1 Null
E14.2	Primary embryonic fibroblast	♀	CIZ1 Null

Table 2.1. Mouse cell lines used for immunofluorescence analysis.

2.1.2 Cell Line Design and Generation

All cells used in this study were generated and gifted by Justin Ainscough. Standard procedures were used to grow all stable cell lines. Mouse (*Mus* musculus) primary embryonic fibroblasts were derived from independent embryos at days 13 to 14 of gestation, with genotype and sex being confirmed as described in Ridings-Figueroa et al. 2017. CIZ1 null mice were generated from C57BL/6 ES clone IST13830B6 (TIGM), harbouring a neomycin resistance gene trap inserted downstream from exon 1. Absence of *Ciz1*/CIZ1 was confirmed as described in Ridings-Figueroa et al. 2017. Breeding and modification of mice was carried out under a UK Home Office license with approval from the Animal Welfare and Ethical Review Body at the University of Leeds. Experimentation on cells derived from the mice was carried out with approval from the Animal Welfare and Ethical Review Body at the University of York.

2.1.3 Media

Unless otherwise stated, mouse primary embryonic fibroblasts (mPEFs) and mouse immortalised embryonic fibroblasts (mEFs; Ridings-Figueroa et al. 2017) were grown in Gibco® Dulbecco's Modified Eagle Medium (DMEM, 11570586, Gibco) with 10% foetal calf serum (PAA) and 1% penicillin/streptomycin with L-glutamine (10378-016, Gibco, formulated to 10,000 Units/ml Penicillin, 10,000 µg/ml Streptomycin, 29.2 mg/ml L-Glutamine).

2.1.4 Maintenance

All primary cells and cell lines were grown at 37 ºC in a humid environment with 5% CO_2 on Nunclon Delta™ cell culture plates (10508921, Thermo Scientific Nunc). Cells were routinely maintained and were passaged when deemed to be near confluency (98% coverage). Passaging was achieved via removal of media, washing with pre-warmed Dulbecco's phosphate buffered saline (D-PBS, 14190-094, Gibco), followed by lifting with 1ml of 0.5% trypsin-ethylenediaminetetraacetic acid (EDTA 10x, 15400-054, Gibco) in D-PBS at 37ºC with 5% CO_2. Trypsin-EDTA was quenched with fresh media and cells were split onto new plates usually at a ratio of 1:3. Cell stocks at relevant passage were harvested in media with 5% dimethyl sulphoxide (DMSO, D5879-100ml, Sigma) and frozen to -80 ºC overnight then stored in liquid N_2.

2.2 Immunofluorescence

Cells were grown on glass coverslips, previously sterilised in ethanol, at 37ºC in a humid environment with 5% CO_2 until ~80% confluency was achieved. Coverslips were treated with 0.1% Triton-X-100 in cytoskeletal (CSK) buffer (10ml Pipes, 20ml NaCl, 102.7g Sucrose, 4ml EGTA, 1ml $MgCl_2$) with 0.01% dithiothereitol (DTT) and protease inhibitor (4693159001, Roche) and were fixed in 4% paraformaldehyde (PFA) for 15 min. Coverslips were rinsed twice with D-PBS, blocked using bovine serum albumin (BSA) antibody buffer (BSA powder, DEPC 10x PBS and 10x detergent mix (4ml 10% SDS, 2ml Tx100), made to 1x with DEPC water) for 30 min, then incubated at 37ºC with 20 µl diluted primary

antibody (Table 2.2) for 120 min in a wetbox. Coverslips were washed twice with BSA antibody buffer, washed once with 3% BSA, then incubated at 37ºC with 20 µl secondary antibody (Table 2.2) for 60 min in the dark in a wetbox. Coverslips were washed three times with BSA antibody buffer, washed once with D-PBS, then mounted onto glass slides with Vectashield containing 0.9 µg/ml 4',6-diamidino-2-phenylindole (DAPI) (H-1200, Vector).

2.2.1 Antibodies

CIZ1 antibodies				
Antibody	**Origin**	**Concentration**	**Secondary antibody**	**Concentration**
1794 (Coverley et al.,2005)	Rabbit polyclonal	1:1000	Alexa Fluor 488 green goat α-rabbit	1:1000
87 (Unpublished, Coverley lab)	Mouse polyclonal	1:20	Alexa Fluor 488 green goat α-mouse	1:1000
Other antibodies				
H3k27me3 (Abcam, ab6002)	Mouse monoclonal	1:2000	Alexa Fluor 568 red goat α-mouse	1:1000
H2AK119Ub1 (CST, D27C4)	Rabbit monoclonal	1:5000	Alexa Fluor 568 red goat α-rabbit	1:1000

Table 2.2. Summary of primary and secondary antibodies used for immunofluorescence analysis.

2.2.2 S Phase Detection via Click-iT® EdU (5-ethynyl-2'-deoxyuridine)

Incorporation of the nucleotide analogue 5-ethynyl-2'-deoxyuridine (Click-iT® EdU Alexa Fluor® 555 nm Imaging Kit, Cat. No. C10338, Invitrogen) was used to visualise newly synthesised DNA at the time of synthesis (pulse) and 30 minutes

after synthesis (chase), allowing determination of cells in S phase. The EdU solution, that contained a thymidine analogue, was diluted to 1 mM from a 10 mM stock using pre-warmed media as per manufacturer's instructions. Cells were grown on glass coverslips as previously described (2.2). Coverslips for the pulse analysis were incubated in 1 ml of media containing 10 μM EdU solution for 30 min. Coverslips for the chase analysis were incubated in 1 ml of media containing 10 μM EdU solution for 30 min then were washed twice with D-PBS, incubated in fresh media for a further 60 min Coverslips were then treated as in section (2.2) with the following modifications: the secondary antibody was applied in conjunction with the Click-iT® reaction cocktail (per coverslip: 17.2 μl 1x reaction buffer, 0.8 μl $CuSO_4$, 0.048 μl Alexa Fluorazaide, 2 μl 1x reaction buffer additive). The slides were kept at 4 ºC in the dark.

2.2.3 S phase Progression inhibition via Thymidine Arrest

Thymidine, a pyrimidine nucleotide, was used to gradually arrest cells throughout S phase via saturation. The thymidine was a kind gift from E. Stewart at 100mM, with a final working concentration of 2.5mM in media. For immunofluorescence analysis, cells were grown on glass coverslips as previously described (2.2). Coverslips were incubated in 500 μl of thymidine for 24 hours. Coverslips for the washout analysis were incubated in 500 μl thymidine for 24 hours, washed twice with D-PBS and then incubated in fresh media for 30 min. Control "cycling" coverslips were incubated in media without the presence of thymidine before experimentation. Coverslips were then treated as in section (2.2). For flow cytometry analysis, thymidine was added to the media in plates on which cells were growing.

2.3 Flow Cytometry

Cells were lifted with trypsin-EDTA as previously described (2.1.4), trypsin-EDTA was quenched with fresh media and cells were pelleted at 10,000 revolutions per minute (rpm) for 5 min. Media was removed, the cell pellet was resuspended and fixed in 70% cold ethanol and then stored at -20ºC until required. Cells were counted using a hemocytometer, pelleted at 13,000 rpm for 5 min, then resuspended in D-PBS so that the concentration of cells was $1x10^6$ cells per 1 ml

D-PBS. Cells were then stained with 10x FACS mix (0.1 mg/ml propidium iodide, 0.4% Triton-X-100, 1x D-PBS) at 100 µl per 1 ml D-PBS at RT for 10 min before being put on ice and analysed. Samples were analysed using a CyAn^{TM} ADP Analyser (Beckman Coulter) and Summit 4.3 software, gated for cells using forward and side scatter.

2.4 Chemical Inhibitors

The DNA polymerase α inhibitor Aphidicolin (Cat. No. A0781, Sigma) was a kind gift from E. Stewart and was used at a working concentration of 5µg/ml with a stock concentration of 1mg/ml solubilised in 0.5% DMSO. The myosin ATPase inhibitor 2-3-Butanedione 2-Monoxime (BDM, Cat. No. 203984, Calbiochem) was used at a working concentration of 20mM in media with a stock concentration of 500mM. The ATPase motor cytoplasmic dynein inhibitor Ciliobrevin D (Cat. No. 250401, Calbiochem) was used at a working concentration of 50µM in media with a stock concentration of 5mM solubilised in 0.2% DMSO. DMSO at 2% had no effect (data not shown), although absence of any effect of an inhibitor solubilised in DMSO is sufficient to conclude the solvent is not having an effect on the assay.

Name	Supplier, ref	Action	Reference(s)
Aphidicolin	Sigma, A0781	Inhibits DNA polymerase α	(Baranovskiy et al. 2014)
2-3-Butanedione 2-Monoxime	Calbiochem, 203984	Inhibits myosin ATPase	(Chuang et al. 2006; Mehta et al. 2010; Kulashreshtha et al. 2016; Stewart et al. 2018)
Ciliobrevin D	Calbiochem, 250401	Inhibits ATPase motor cytoplasmic dynein	(den Hollander and Kumar 2006)

Table 2.3. Inhibitors used for Xi relocation mechanistic analysis.

2.5 Microscopy

Coverslips processed for immunofluorescence, including those for EdU detection and chemical inhibitor analysis, were imaged using a Zeiss Axiovert 200M inverted light microscope with a x64/40 oil immersion objective. Images were taken using an AxioCam HRm digital camera and Openlab acquisition software (Perkin Elmer). Images were manipulated using Affinity Photo 1.5.2 and Fiji ImageJ software (Schindelin et al. 2012).

2.6 Scoring and Positional Classification

Routinely ~30% of cells within a cycling population incorporate EdU during the pulse labelling period, with ~10% of these having a replicating Xi (condensed EdU patch within a cell with an early or mid-S phase replication pattern) as confirmed by co-staining with CIZ1 (Appendix A; Stewart et al. 2018). For Xi positional information via EdU detection, at least 100 cells in S phase (EdU stained) per coverslip were scored per condition. The location of the EdU-labelled CIZ1-marked Xis were categorised as either “internal” or “peripheral”, based upon a binary classification that was maintained throughout (Figure 4.1C). Xis were scored as internal if all of the patch, including all foci, was within and not in contact with the outer membrane of the nuclei. Xis were scored as peripheral if any part of the patch or individual foci was in contact with the outer membrane of the nuclei, often confirmed by comparison with DAPI staining. For positional information via thymidine arrest, at least 50 cells with a replicating Xi (confirmed via CIZ1 and H2AK119Ub co-staining) per coverslip were scored per condition (with one exception being 20 cells). The location of CIZ1/H2AK119Ub-marked Xi’s were categorised as either “internal” or “peripheral” based upon the same binary classification that was used for EdU incorporation. For area information via thymidine arrest, at least 20 cells with a replicating Xi per coverslip were quantified per condition. In all cases, only cells with one replicating Xi were used. Cells with two or more replicating Xi’s were ignored.

2.7 Instructions for area quantification

Use of “Area.macro” is described in more detail below. In brief, “Area.macro” splits the image into three channels (red, green and blue, for H2AK119Ub, CIZ1 and DAPI respectively), selects a region(s) of interest (ROIs) on the first channel image based on the “Otsu Threshold” and applies this threshold producing a mask image with ROIs and area measurements numbered to allow cross checking. This can then be done for the second channel image and the third channel image.

To manually perform the same steps as “Area.macro” follow the instructions below:

Open file in imageJ
Image: Colour: Split channels
Image: Adjust: Threshold..
Open drop down menu and select “Otsu” (Otsu, 1979)

Apply
Process: Binary: Convert to Mask
Analyse: Analyse particles..
In dialogue box, Size: 0-infinity, Pixel units unticked, Circularity: 0.00-1.00, Show: Nothing, only Display results and Add to Manager ticked
This produces area measurements for labelled ROIs. Repeat these steps for each of the colour channels.

Both area measurements for CIZ1-marked Xis and nuclei (DAPI staining) were copied onto an Excel spreadsheet. Percentage area of the nucleus occupied by CIZ1 was then calculated.

2.8 Statistical Analysis

All graphs were produced in Microsoft Excel. Area quantifications were carried out in Fiji ImageJ using a pre-made macro to ensure consistency. Statistical tests were carried out in Microsoft Excel and R, with significant p values being: *P≤0.05, **P≤0.01, ***P≤0.001).

Chapter 3. The role of CIZ1 in Polycomb complex function at the Xi

3.1 Introduction

Trimethylation of histone 3 at lysine 27 (H3K27me3) by EZH2 (subunit of PRC2) (Margueron and Reinberg 2011) and monoubiquitination of histone 2A at lysine 119 (H2AK119Ub1) by RING1a/b (subunit of PRC1) (de Napoles et al. 2004; Fang et al. 2004) are both involved in the process of X chromosome inactivation as epigenetic transcriptional repressors. Previous data has not only shown that enriched marks of H3K27me3 co-localise with CIZ1 staining in wild type cells, but also that these enriched marks are lost when CIZ1 is absent (Ridings-Figueroa et al. 2017).

3.2 Aims

The aim of the work described here was to determine the behaviour of both H3K27me3 and H2AK119Ub1 chromatin modifications in:

i) Wild type primary cells
ii) CIZ1 null primary cells
iii) Wild type culture adapted populations
iv) CIZ1 null culture adapted populations

3.3 Experimental Procedure

Immunofluorescence (Methods 2.2) was used to visualise enriched marks of H3K27me3 and H2AK119Ub1 in both wild type and CIZ1 null embryonic fibroblast populations, using anti-H3K27me3 polyclonal antibody and anti-H2AK119Ub1 polyclonal antibody respectively (Methods 2.2.1, Table 2.2). Anti-CIZ1 antibodies (Methods 2.2.1, Table 2.2) allowed determination of the Xi in wild type cells. Protein level analysis of EZH2, responsible for H3K27me3 modification, was previously carried out via Western blot (Appendix B; Turner 2017) and was expanded upon using statistical analysis.

3.4 Results

3.4.1 CIZ1 is required for enrichment of chromatin modifications at the Xi

As expected, evaluation of both H3K27me3 and H2AK119Ub1 in a population of wild type primary cells (E13.1) revealed the presence of enriched marks for both chromatin modifications at the Xi, with 93% of cells (280/301 cells) showing an enriched H3K27me3 mark and 96% of cells (191/200 cells) showing an enriched H2AK119Ub1 mark (Figure 3.1). Conversely, detection in a population of CIZ1 null primary cells (E13.15) revealed the absence of enriched marks for both chromatin modifications, with only 2% of cells (2/100 cells) showing an enriched H3K27me3 mark and 4% of cells (4/100 cells) showing an enriched H2AK119Ub1 mark (Figure 3.1). This result is consistent with and further expands upon previous data, adding to the hypothesis that CIZ1 is required for polycomb repressive complex function at the Xi. Overall staining of both H3K27me3 and H2AK119Ub1 across the whole nucleus did not appear to differ dramatically.

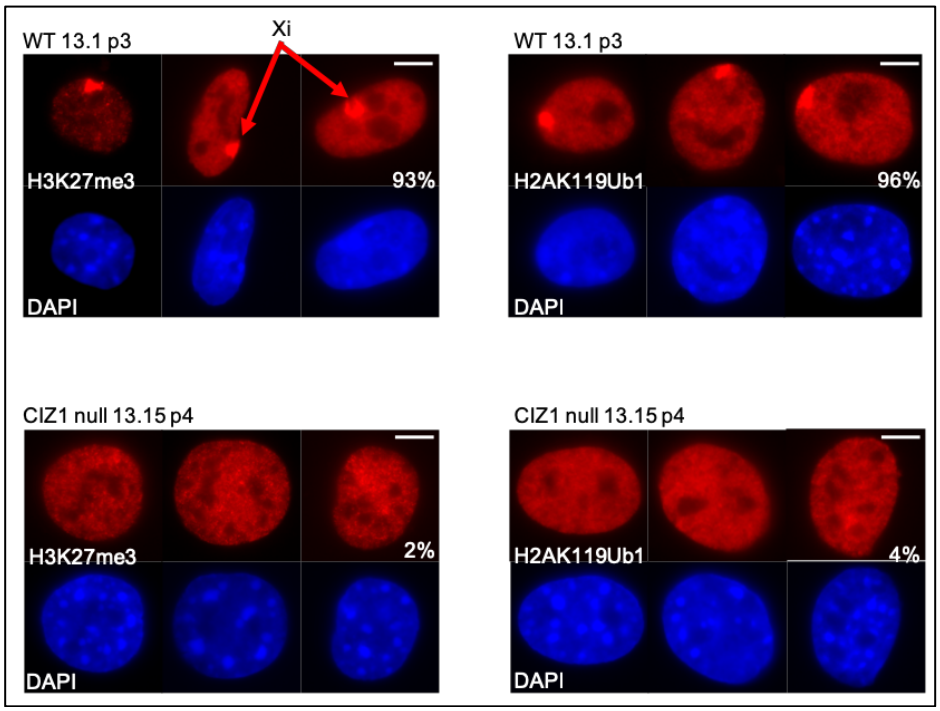

Figure 3.1. Polycomb repressive complex function in CIZ1 null cells.
Example images of wild type primary embryonic fibroblasts (E13.1 p3) and CIZ1 null primary embryonic fibroblasts (E13.15 p4) immuno-stained for H3K27me3 (left) and H2AK119Ub1 (right). Percentage of nuclei within the population where Xi is marked by the chromatin modifications are shown. Both H3K27me3 and H2AK119Ub1 patches are present in wild type primary embryonic fibroblasts, but are absent in CIZ1 null primary embryonic fibroblasts, linking CIZ1 with PRC function. H3K27me3 and H2AK119Ub1 are red, DNA is blue, bar is 5 microns, arrows show example Xis.

3.4.2 Re-emergence of enriched marks and altered expression of polycomb repressive complex upon culture adaptation

An important question to ask was whether chromatin modifications are affected upon culture adaptation. Culture adapted lines derived from independent wild type and CIZ1 null embryos were tested for H3K27me3 and H2AK119Ub1. In wild type culture adapted populations, H3K27me3 and H2AK119Ub1 were present at the Xi in 95% of cells (476/500 cells) and 92% of cells (549/600 cells) respectively (Figure 3.2A). Surprisingly, in CIZ1 null culture adapted populations, a re-emergence of both chromatin modifications was seen. 23% (185/800 cells) and 39% (195/500 cells) of E13.15 and E13.17 cells respectively showed an enriched H3K27me3 mark, and 26% (158/600 cells) and 37% (110/300 cells) of

E13.15 and E13.17 cells respectively showed an enriched H2AK119Ub1 mark (Figure 3.2A, 3.2B). The re-emergence of enriched H3K27me3 marks was very unexpected but was also very reproducible, promoting further questions regarding the behaviour of the chromatin modifications upon culture adaptation.

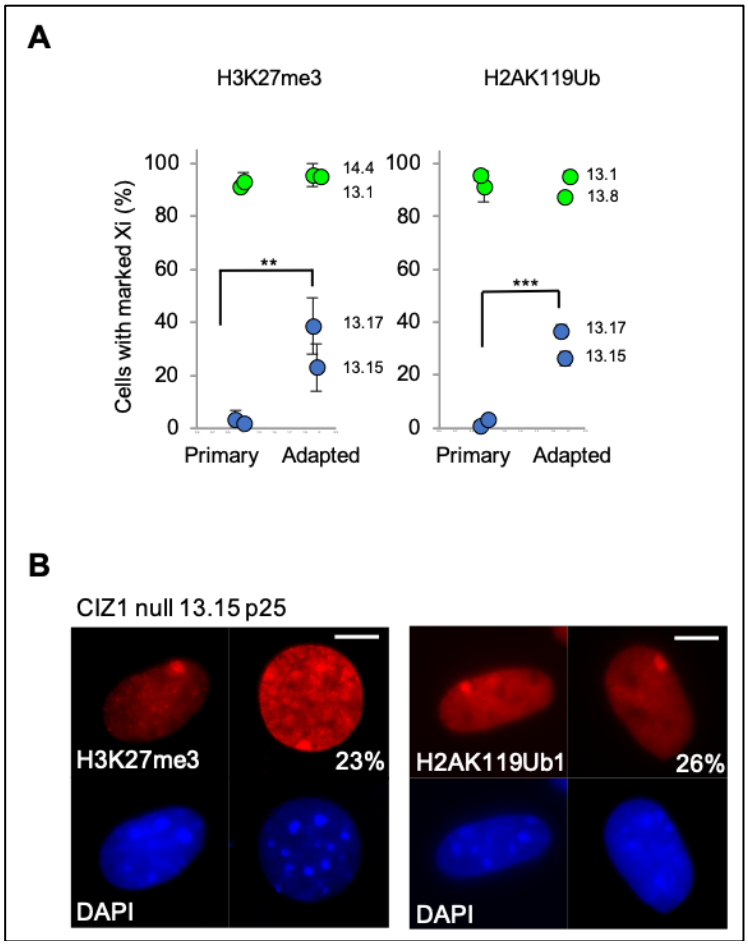

Figure 3.2. PRC chromatin modifications in primary and culture adapted wild type and CIZ1 null cells.

A) Proportion of primary (<p4) and culture adapted cells (>p9) with H3K27me3 marked Xis (left) and H2AK119Ub1 marked Xis (right), in wild type (green) and CIZ1 null (blue) genotypes, ±SEM from triplicate analyses for each cell line. Re-emergence of marked Xis in CIZ1 null cells occurs upon culture adaptation, compared by students t-test. For all analysis *P≤0.05, **P≤0.01, ***P≤0.001. B) Representative example images of culture adapted CIZ1 null nuclei immune-stained for H3K27me3 (left) and H2AK119Ub1 (right). Percentage of nuclei within the population where Xi is marked by the chromatin modifications are shown. Reemergence of enriched marks occurs upon culture adaptation in CIZ1 null populations. H3K27me3 and H2AK119Ub1 are red, DNA is blue, bar is 10 microns.

Another way to test the behaviour of the marks would be via western blot. Interestingly, protein level analysis of EZH2, the catalytic subunit of PRC2, in primary wild type and CIZ1 null cell lysates revealed two different isoforms of EZH2, (reproduced from Turner 2017; Figure 3.3A). The upper form (designated EZH2p for “primary”) was seen to be more dominant in wild type primary cells whereas the lower form (designed EZH2α) was seen to be more prevalent in CIZ1 null primary cells than in wild type primary cells (Figure 3.3B). Furthermore, the dominant EZH2p form in wild type cells was replaced by the EZH2α form upon culture adaptation, accompanied by an increase in level (Figure 3.3C). The same was evident in CIZ1 null cells with progression to culture adaptation.

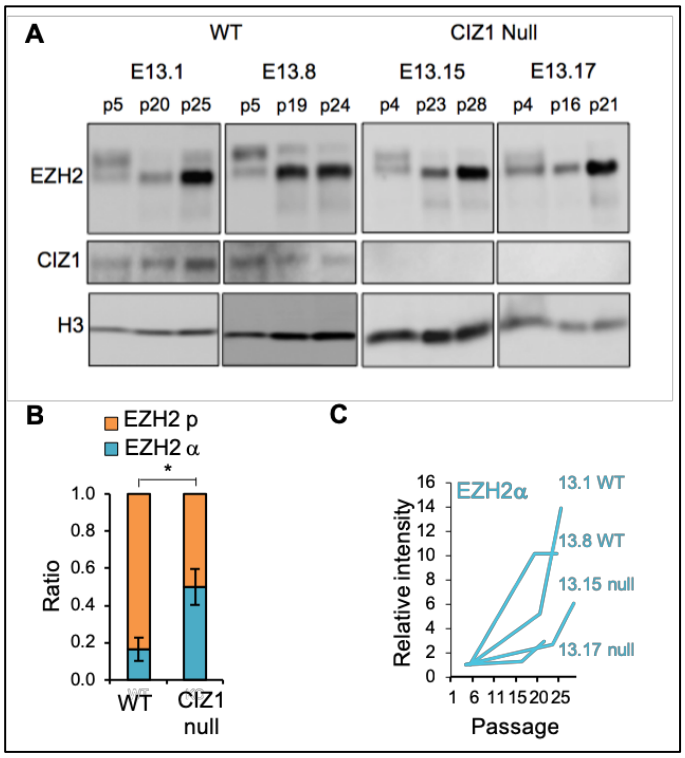

Figure 3.3. EZH2 protein level expression in primary and culture adapted cells. A) Western blot showing EZH2 (PRC2 catalytic subunit), CIZ1 and histone H3 in primary embryonic fibroblasts and culture adapted populations of wild type and CIZ1 null genotypes. There are two isoforms of EZH2 in primary cells (classified as “p” and “α”). Reproduced from Turner 2017. B) Quantification of EZH2 isoform “p” and “α” ratio in wild type and CIZ1 null primary cells from Figure 3.3A, showing mean data ±SEM for three independent populations of each genotype (wild type = 13.1, 13.8, 14.4. CIZ1 null = 13.15, 13.17, 14.2), compared by students t-test. C) Intensity quantification of EZH2α in primary cells and culture adapted populations after normalization to H3. EZH2 level increases with passage, irrespective of genotype.

3.5 Discussion

Results described here further validated and strengthen previous conclusions, that were based on a limited number of cells (Ridings-Figueroa et al. 2017), clearly demonstrating the presence of enriched H3K27me3 marks in wild type primary cells and the absence of the marks in the absence of CIZ1. This has been extended by inclusion of the chromatin modification laid down by PRC1, H2AK119Ub1. As expected, enriched H2AK119Ub1 marks were present in wild type primary cells and absent in CIZ1 null primary cells, demonstrating that CIZ1 is required for the normal function of both polycomb repressive complexes at the Xi. As a result of the loss of both chromatin modifications CIZ1 null cells, one would expect chromatin to remain active resulting in unwanted expression of X-linked genes at the Xi, although this has not been tested experimentally. Previous work also showed that the loss of CIZ1 resulted in a general reduction in the intensity of H3K27me3 staining in the rest of the nucleus (Ridings-Figueroa et al. 2017), suggesting that the consequence of loss of CIZ1 may be more universal instead of Xi specific. Data produced here was not consistent with this, showing no clear difference between general H3K27me3 signal in wild type and CIZ1 null cells. It is possible that cell handling, cycling rate or differences in protocol are contributory factors. Western blot analysis of H3K27me3 would help resolve this. Intriguingly, marks for both chromatin modifications begin to re-emerge in CIZ1 null populations during culture adaptation. This unexpected result suggests that the absence of the chromatin modifications, as a result of the absence of CIZ1, is reversed or counteracted by culture adaptation in a compensatory manner.

Regarding protein level analysis, culture adaptation of wild type cells was identified as a driver of a shift in EZH2 form. Validation of these two forms of EZH2 (p and α) is crucial and is currently being investigated further. Adding to this, culture adaptation was also identified as a driver of an increase in relative intensity of the lower form of EZH2. It is possible that this increase in EZH2 is responsible for the re-emergence of enriched H3K27me3 marks seen in CIZ1 null cells. It would be important to test whether this increase in EZH2 intensity is seen in cells via immunofluorescence, adding to the validity of the result seen by Western blot. It would also be of interest to investigate the PRC1 subunit RING1a/b, comparing relative levels in primary and culture adapted wild type

cells by immunocytochemistry and Western blot. This would aid testing the hypothesis that increased enzyme levels drives re-emergence of chromatin modifications.

Chapter 4. Exploiting the EdU (5-ethynyl-2'-deoxyuridine) assay to study the location of the inactive X chromosome during S phase

4.1 Introduction

As previously described, the inactive X chromosome (Xi) is normally located at the nuclear periphery, anchored via lamin B receptor (Chen et al. 2016). Furthermore, it has been suggested that the Xi transiently visits the perinucleolar zone during S phase in a dynamic process that allows maintenance of epigenetic modifications (Zhang et al. 2007). It is of importance to expand upon this previously published data, in order to aid in the understanding of the function of CIZ1. Incorporation of the nucleotide analogue EdU (Figure 4.1A) has previously been used to identify and visualise Xis undergoing DNA replication in mid S phase (Casas-Delucchi et al. 2011).

4.2 Aims

The aim of the work described in this chapter was to further investigate the location of the Xi during S phase in:

i) Wild type primary mouse embryonic fibroblasts
ii) CIZ1 null primary mouse embryonic fibroblasts
iii) Wild type culture adapted mouse embryonic fibroblast populations

4.3 Experimental Procedure

Incorporation of the modified base EdU (Methods 2.2.2) into cells allowed visualisation of DNA at the time of Xi replication (pulse) and after Xi replication (chase). Replicating Xi were visible based on the pattern of EdU incorporation (Appendix A; Stewart et al. 2018), confirmed by co-localisation of the high intensity EdU patch with CIZ1 (Figure 4.1B). The location of the EdU-labelled

CIZ1-marked Xis were categorised as either “internal” or “peripheral” based upon a binary classification that was maintained throughout (Figure 4.1C).

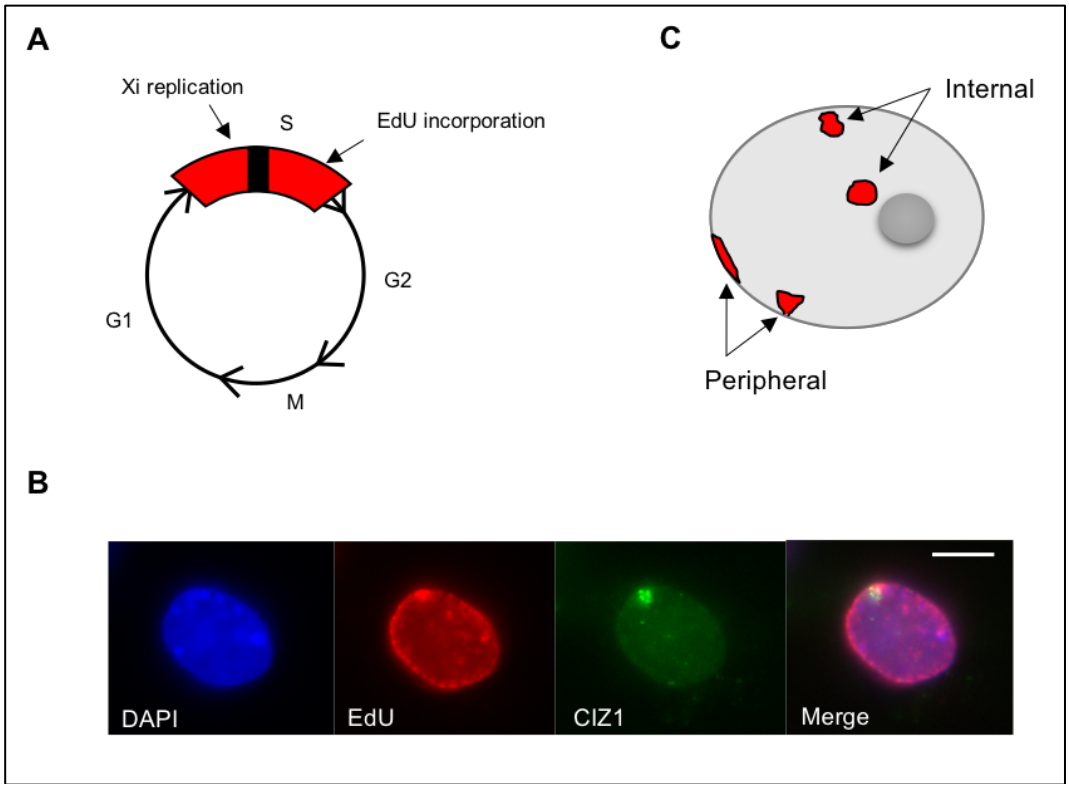

Figure 4.1. Principles of EdU Assay for detection of cells in the process of replicating their Xi.

A) Schematic representation of the cell cycle showing incorporation of nucleotide analogue EdU during S phase, allowing visualization of the replicating Xi during S phase. B) Verification of the identify of EdU-Xi by co-staining for CIZ1 (green), using anti-CIZ1 polyclonal antibody 1794 (Coverley et al., 2005). DNA is blue, bar is 10 microns. C) Schematic showing binary classification of Xi location (peripheral or internal) at the time of (pulse) or after (chase) incorporation of EdU.

4.4 Results

4.4.1 Xi changes location during DNA replication in primary cells

Three populations of primary cells isolated from independent wild type embryos (E14.4, E13.1 and E13.8) underwent EdU staining with separate coverslips being subjected to a pulse and a chase period (Figure 4.2A). At the time of Xi replication/EdU incorporation, CIZ1-marked EdU-labelled Xis were mainly found to be located towards the interior of the nuclei (Figure 4.2B), whereas after Xi replication, Xis were mainly found to be located at the periphery of the nuclei (Figure 4.2B). This result is consistent with the suggestion that the Xi transiently visits the perinucleolar zone during S phase, moving back to the nuclear periphery within 60 minutes. This movement was seen in all three populations of wild type primary cells, each of which had three technical replicates counting ~100 nuclei in the window of S phase when the Xi is replicating (Figure 4.2C), allowing interpretation of Xi movement in wild type primary cells (Figure 4.2D). The function of and requirements for this movement will be addressed in later chapters. At this point it is of importance to distinguish the common nomenclature that will be used when describing both the inward and outward movement of the Xi during S phase. Thus, I propose the inward movement of the Xi to be known as “departure” and the outward movement to be known as “return” (Figure 4.2E).

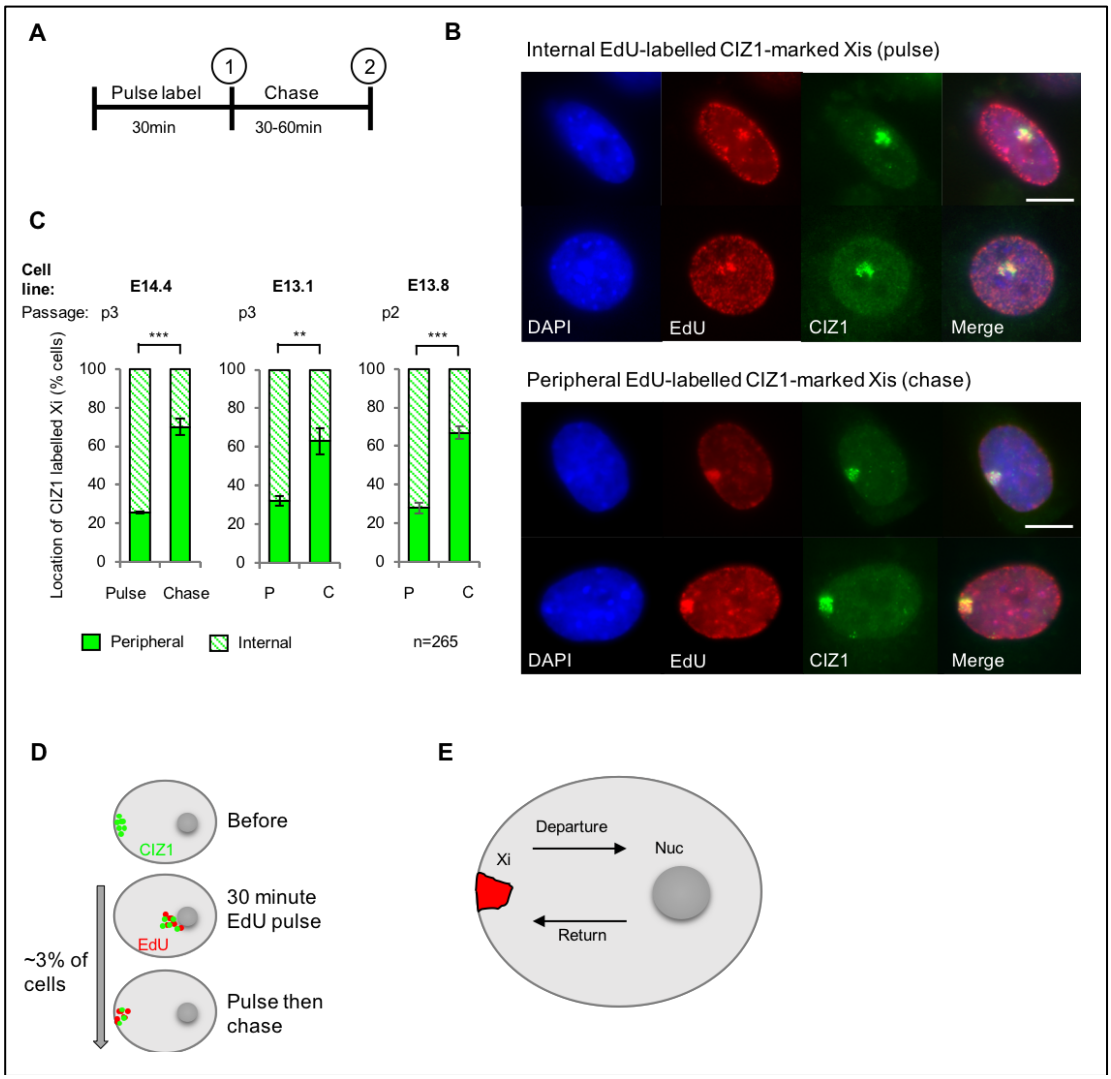

Figure 4.2. Location of replicating Xi in primary wild type cells.

A) Timeline of EdU assay, comparing the location of Xi at time points 1 (immediately after 30 minutes of labelling with EdU) and 2 (after a further chase period with no further labelling). B) Example images of wild type primary cell nuclei stained for EdU (red) and CIZ1 (green) showing internal and peripheral Xis. DNA is blue, bar is 10 microns. C) Location of CIZ1-marked and EdU-labelled Xis (3-5% of the population) in three independent wild type primary embryonic fibroblast populations (cell lines and passage numbers indicated) at time points 1 and 2. *P≤0.05, **P≤0.01, ***P≤0.001. n=total nuclei with replicating Xi scored. D) Model interpreting the change in average location of CIZ1-marked and EdU-labelled Xis between time points 1 and 2, as movement towards the nuclear interior and back to the nuclear periphery. E) Graphical model depicting proposed nomenclature for Xi inward movement (departure) and outward movement (return).

4.4.2 CIZ1 is required for Xi movement in primary cells

Naturally, the follow up to this was to determine whether CIZ1 was required for the internalisation of the Xi seen in wild type primary cells. In order to address this, the same experiment as above was repeated on CIZ1 null cells. Three independent primary CIZ1 null populations (E13.15, E13.17 and E14.2, Methods 2.1.1, Table 2.1) underwent EdU staining with separate coverslips being subjected to a pulse and a chase period. In all three of the primary CIZ1 null populations no significant difference was found between the position of the Xi immediately after a 30 minute pulse labelling window compared to after a chase period (Figure 4.3A). Overall, the Xi showed a preference for the nuclear periphery in 61% of pulse cells and 62% of chase cells (Figure 4.3A, 4.3B). When data averaged for these three primary CIZ1 null populations was compared to data averaged for the three primary wild type populations (Figure 4.2C), there was a clearly significant difference between the position of the Xi during synthesis, with 30% less internal Xis in the absence of CIZ1 (Figure 4.3C). Therefore, this suggests that the departure of the Xi from the nuclear periphery in CIZ1 null cells is compromised.

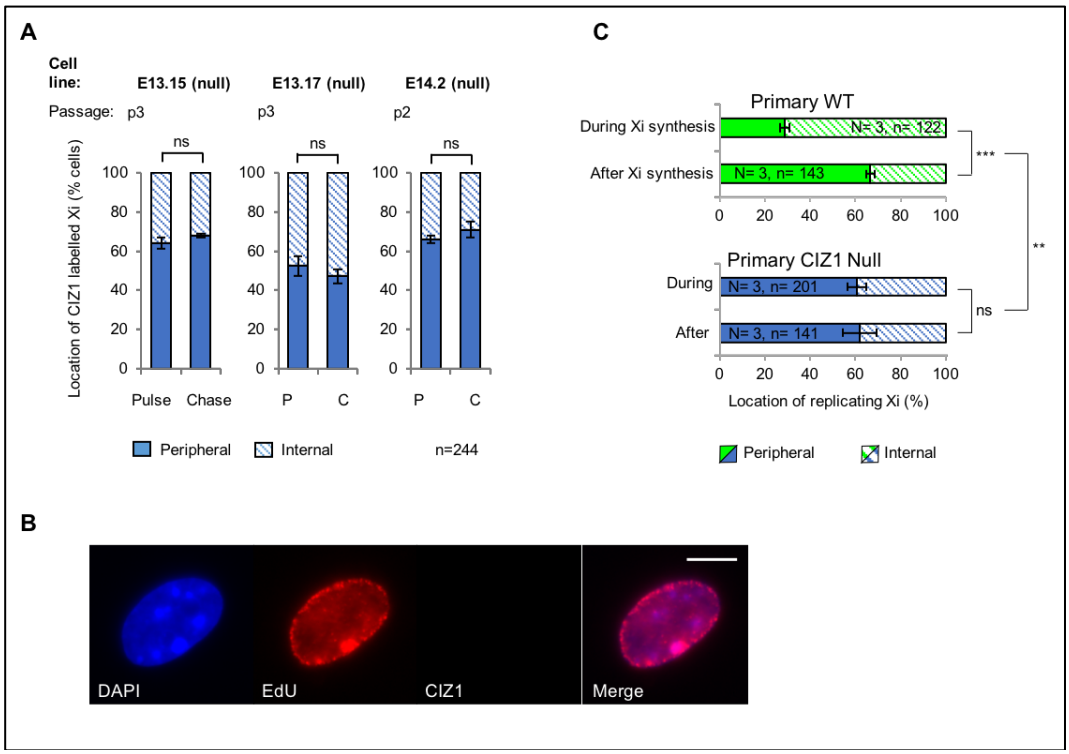

Figure 4.3. Location of replicating Xi in primary CIZ1 null cells.

A) Location of EdU-labelled Xi in three independent CIZ1 null primary embryonic fibroblast populations (cell lines and passage numbers indicated) at time points 1 and 2 (Figure 4.2A). Average Xi position remains unchanged, compared by student's t-test. B) Representative example image of CIZ1 null primary cell nucleus with replicating Xi stained with EdU (red) and CIZ1 (no label). DNA is blue, bar is 10 microns. C) Mean data ±SEM for all three wild type primary embryonic fibroblasts (from Figure 4.2C) and all three CIZ1 null primary embryonic fibroblasts, compared by ANOVA. For all analysis *P≤0.05, **P≤0.01, ***P≤0.001. N=independent cell lines, n=total nuclei with replicating Xi scored.

4.4.3 Movement mechanism is prone to degeneration upon culture adaptation

Another important question was whether Xi movement seen in primary populations occurs in cell lines. Culture adapted lines derived from all three parent populations used in the primary population analysis (E14.4, E13.1 and E13.8) underwent EdU staining as above. In two out of the three culture-adapted lines (E13.8 and E14.4) there was no significant difference between the position of the Xi immediately after a 30 minute pulse labelling window compared to after a chase period (Figure 4.4A), with Xi in both showing a preference for the nuclear

periphery under both conditions (Figure 4.4B), mimicking what was seen in primary CIZ1 null populations. In the third culture adapted cell line (E13.1) the Xi had a far reduced preference for the nuclear interior after the pulse-labelling window when compared to the parent primary population (comparing Figure 4.4A to Figure 4.2C). When data averaged for the three culture adapted populations was compared to data averaged from the parent primary populations, there was a significant difference between the position of the Xi during synthesis, with a 27% decrease in the percentage of internal Xis (Figure 4.4C). Therefore, this suggests that, like in primary CIZ1 null populations, the departure of the Xi from the nuclear periphery in culture adapted populations is prevented.

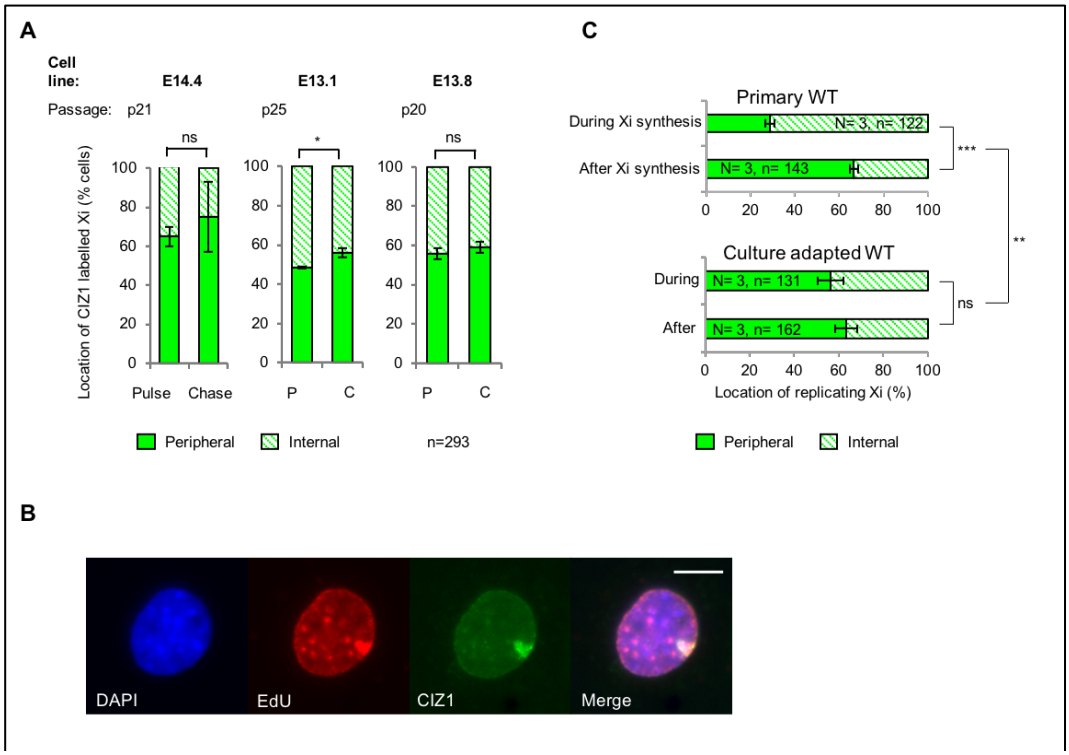

Figure 4.4. Location of replicating Xi in culture adapted wild type cells.
A) Location of CIZ1-marked and EdU-labelled Xi in three wild type culture adapted cell lines (passage numbers indicated) at time points 1 and 2 (Figure 4.2A). Average Xi position remains unchanged, compared by student's t-test. Data for E13.1 p25 was generated by Victoria Scott. B) Representative example image of wild type culture adapted nucleus with replicating Xi stained with EdU (red) and CIZ1 (green). DNA is blue, bar is 10 microns. C) Mean data ±SEM for all three wild type primary embryonic fibroblasts (from Figure 4.2C) and all three wild type culture adapted populations, compared by ANOVA. For all analysis *P≤0.05, **P≤0.01, ***P≤0.001. N=independent cell lines, n=total nuclei with replicating Xi scored.

4.5 Discussion

Experiments described here confirm that the Xi occupies two distinct regions within a nucleus, similar to those seen in the very first description (Barr and Bertram, 1949). Furthermore, experiments confirm dynamic movement of the Xi towards the nuclear interior during S phase in primary wild type populations followed by a relocation back to the nuclear periphery after Xi synthesis, the function and requirements of which will be addressed in later chapters. As seen, not all replicating Xis are located towards the nuclear interior immediately following a pulse-labelling window. Possible explanations include (i) incorporation of EdU near the end of the Xi DNA synthesis window, after the Xi has returned to the nuclear periphery and (ii) nucleoli located towards the nuclear periphery, negating requirement for long distance chromatin movement. The results also suggest that CIZ1 plays a role in the Xi movement mechanism during S phase, as the loss of CIZ1 results in the loss of Xi movement. There is no evidence that the loss of CIZ1 affects replication timing, coordination of Xi replication or S phase pattern (Stewart et al. 2018; Coverley et al. 2005), therefore this loss in movement is likely to be dependent upon CIZ1. This is the first instance that CIZ1 has been suggested to be involved in chromosomal movement. It is, however, possible that absence of CIZ1 results in the replicating Xi spending more or less time in the nuclear interior, therefore causing a change in positional scoring due to missing the time at which the Xi departs from the nuclear periphery. This could be addressed using a detailed pulse-labelling time course, although at this point it is not unreasonable to conclude that Xi movement is compromised.

Scepticism and criticism may arise regarding the method of classification of positional location of replicating Xis (internal or peripheral based upon visual determination). Although visual determination is not always reliable, the binary classification was kept throughout all experiments with great stringency. An alternative approach is to computationally calculate the position of the Xi along the average nuclear radius and then define the Xi as internal or peripheral based on the distance ratio. This method was not adopted as, although near identical results are generated (in twice the time), all non-spherical nuclei have to be excluded from the analysis. This applies to many of the nuclei within a population. Thus, I elected to stand by visual binary classification.

Xi departure from the nuclear periphery was also compromised in all culture adapted cell lines studied here, producing results similar to those of CIZ1 null primary cells. As with the CIZ1 null cells, no difference was found in the timing of replication between primary wild type and culture adapted wild type cells, with over 80% of cells showing a replicating CIZ1-labelled Xi in early/mid S phase (Stewart et al. 2018). Therefore, this suggests that the compromised movement seen in the culture adapted cells occurs independently of CIZ1, and that the mechanism by which the Xi relocates during replication is susceptible to degeneration with progression to a culture adapted state. This further implies that established cell lines do not accurately represent the state of cells in the body. As one would expect, there are differences between cell lines, namely the E13.1 cell line showing a reduced loss of Xi movement upon culture adaptation when compared to the E13.8 and E14.4 cell lines. Interestingly, Xi movement is gradually lost instead of a sudden halt (Appendix C). It is likely that the relocation capability is lost at different rates between different cell lines due to epigenetic factors, such as different proliferation rates possibly as a result of a growth advantage, rather than a mutational change. Another possibility is that there are different populations of cells within the primary cultures with different proliferation rates that are gradually out competed over time. Analysis of more intermediate passages between primary cells and culture adapted cells (p6, p7, p8, etc) would be required to test this hypothesis and validate a gradual loss of Xi relocation. Furthermore, the result of the E13.1 cell line upon culture adaptation is highly reproducible, showing similar results in all three technical replicates which were from different stock vials at different times. Therefore, it is plausible to conclude that the reduced loss of Xi movement shown by the E13.1 cell line remains a significant observation.

Analysis carried out in this study consisted of 2-Dimensional microscopy. Although results regarding the location of Xis to the nuclear membrane were visually clear when following the binary classification, it is possible that some peripheral Xis were missed. Utilizing specific fluorescent probes and confocal microscopy to take images of optical sections through cells to visualise the cells in 3-Dimensions would provide a more definitive method of scoring true Xi location relative to the nuclear membrane. However, currently no discussion has

taken place regarding this possibility due to the time consuming and expensive nature of the process. Moreover, the percentage of peripheral Xis missed is likely to be small enough to not significantly change the results obtained.

In this chapter, two different drivers of loss of Xi movement have been identified: 1) CIZ1 and 2) an unknown driver in culture adapted wild type cells, both of which will be expanded upon in the following chapter.

Chapter 5. Using chemical inhibitors to investigate the mechanism of Xi departure and return

5.1 Introduction

Having identified dynamic movement of the Xi to the nucleolus and back during S phase, naturally, the follow up question concerned understanding the requirements of this movement. To investigate this, incorporation of specific chemical inhibitors (Table 2.3) at the time of both the departure of the Xi and the return of the Xi was adopted. Aphidicolin (Sigma, A0781), 2-3-Butanedione 2-Monoxime (BDM, Calbiochem, 203984) and Ciliobrevin D (Calbiochem, 250401), either alone or in combination, were used in this study.

5.1.1 Rationale for inhibitor selection

The DNA polymerase α inhibitor Aphidicolin binds at the active site of polymerase α causing a rotation of the template guanine, blocking the binding of dCTP (deoxycytidine triphosphate) (Baranovskiy et al. 2014). Inhibition with Aphidicolin would investigate whether ongoing DNA synthesis was required. BDM inhibits nuclear myosin function. Nuclear myosin 1 (NM1), a chromatin-bound motor protein (Pestic-Dragovich et al. 2000), has previously been implicated in the process of chromosomal movement and compartmentalisation, although very little is known mechanistically. Tagged loci and live cell imaging approaches in CHO cells showed long-range translocation of a specific chromosomal site from the nuclear periphery to the interior following transcription activation (Chuang et al. 2006). This translocation was seen to be blocked by BDM, allowing the suggestion that NM1 may also be required for Xi relocation. Additional findings show that NM1 is also involved in chromosome territory relocation in primary human fibroblasts (Mehta et al. 2010) and during DNA damage response (Kulashreshtha et al. 2016). Furthermore, work carried out in the Coverley lab has shown that NM1 is consistently down regulated upon culture adaptation (Stewart et al. 2018), thus providing a suggestion as to why Xi departure is lost. Therefore, inhibition with BDM would investigate whether Xi relocation requires nuclear myosin function. Ciliobrevin D, an ATPase motor cytoplasmic dynein inhibitor, disrupts spindle pole focusing and kinetochore-microtubule attachment

(Firestone et al. 2012). Dynein light chain 1 (DLC1) is a cytoplasmic dynein that has been shown to be involved in retrograde intracellular transport along microtubules (Paschal and Vallee 1987; Schroer et al. 1989). Interestingly, DLC1 has more recently been found to be a direct binding partner of CIZ1, with the interaction being responsible for an increase in CDK2 activity, accelerating S phase progression (den Hollander and Kumar 2006). It is possible to hypothesize that the retrograde action of DLC1 is linked with CIZ1 attachment, thus providing another suggestion as to why Xi departure is lost. Therefore, inhibition with Ciliobrevin D would investigate whether Xi relocation requires cytoplasmic dynein function.

5.2 Aims

The aim of the work described in this chapter was to determine the requirements of Xi departure and return through the inhibition of specific pathways, using aphidicolin, BDM, Ciliobrevin D and a combination of BDM and Ciliobrevin D.

5.3 Experimental Procedure

These questions were addressed by modification of the EdU pulse/chase protocol (Methods 2.2.2), allowing development of a strategy to test Xi relocation requirements. Modification involved a 30 minute incubation with media containing the inhibitor prior to pulse labelling in order to test requirements of Xi departure (Figure 5.1, pathway 1), and a 30 minute chase period with media containing the inhibitor in order to test requirements of Xi return (Figure 5.1, pathway 2).

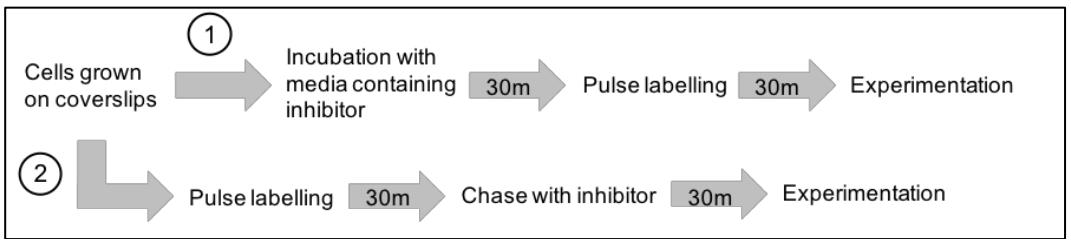

Figure 5.1. Strategy for evaluation of the requirements of Xi relocation.
Timeline for modification of EdU protocol allowing evaluation of requirements of Xi departure (pathway 1) and Xi return (pathway 2).

5.4 Results

5.4.1 What are the requirements of Xi departure and return?

Three populations of primary cells isolated from independent wild type embryos (E14.4, E13.1 and E13.8) underwent modified EdU staining with the addition of each inhibitor. Although it was not possible to test the requirement of ongoing DNA synthesis for Xi departure (as EdU pulse labelling was coincident with the window of DNA synthesis), incorporation of aphidicolin before the pulse did allow confirmation of aphidicolin activity as no EdU incorporation occurred in its presence (Figure 5.2A). Introduction of aphidicolin during the chase period, however, did enable testing of whether ongoing DNA synthesis was required for Xi return. Following a 30 minute chase period with media containing aphidicolin, CIZ1-marked EdU-labelled Xis were predominantly located at the nuclear periphery (Figure 5.2B), with no significant difference between the average Xi location compared to the average Xi location after the control chase (Figure 5.2C). Thus, DNA synthesis does not appear to be required for return.

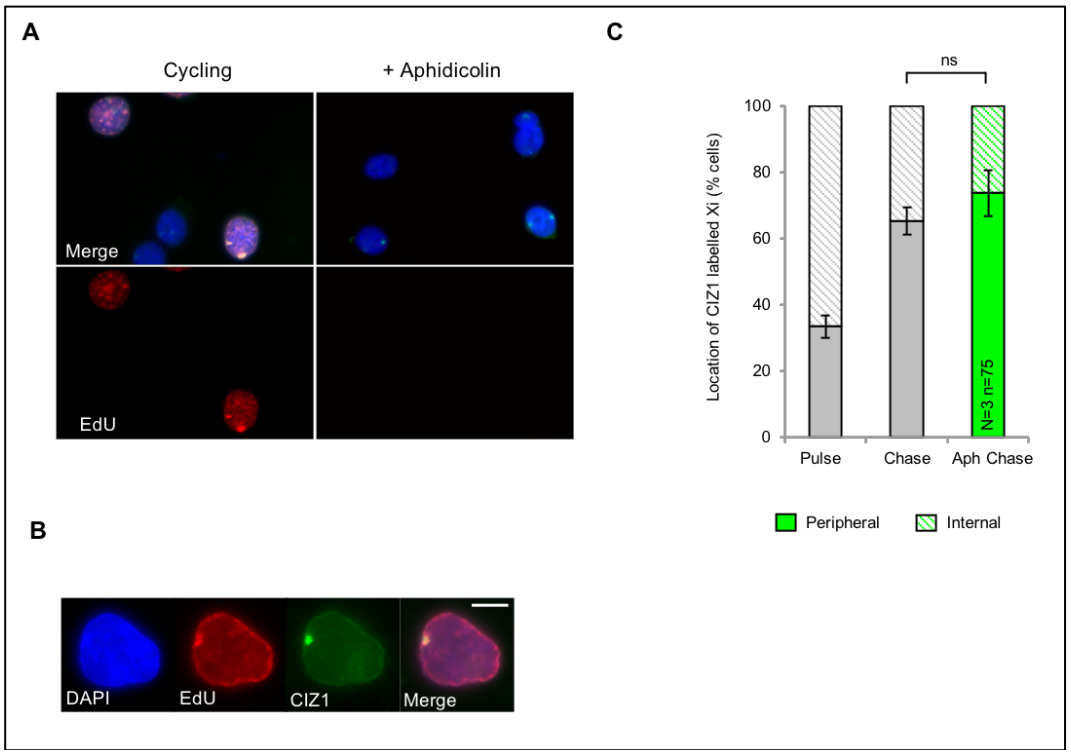

Figure 5.2. Ongoing DNA synthesis is not required for return to the nuclear periphery.

A) Representative images of wild type primary nuclei cycling population (left) and following incubation with aphidicolin (right). Aphidicolin blocks EdU incorporation. B) Representative example image of wild type primary nucleus after a chase period in the presence of Aphidicolin, with replicating Xi, stained with EdU (red) and CIZ1 (green). DNA is blue, bar is 10 microns. C) Mean data ±SEM for location of CIZ1-marked and EdU-labelled Xi for wild type primary embryonic fibroblasts after chase period (grey), compared to after a chase period in the presence of Aphidicolin (green). Average Xi position is no different, compared by students t-test. *P≤0.05, **P≤0.01, ***P≤0.001. N=independent cell lines, n=total nuclei with replicating Xi scored.

BDM was introduced both prior to the EdU pulse labelling window and during the chase period to test if nuclear myosin function was required for Xi departure or return. A clear significant difference was seen between the average location of CIZ1-labelled EdU-marked Xis after a 30 minute incubation with BDM compared to the average Xi location of the pulse control (Figure 5.3A, 5.3B). The percentage of internally located Xis decreased to 44% following incubation with BDM compared to 67% in the control pulse. A significant difference was also seen between the average location of Xis after a 30 minute chase with media

containing BDM compared to the average Xi location after the control chase (Figure 5.3A, 5.3C), with the percentage of peripheral Xis decreasing to 51% compared to 65% in the control chase. These results suggest that nuclear myosin function is required for both Xi departure and return.

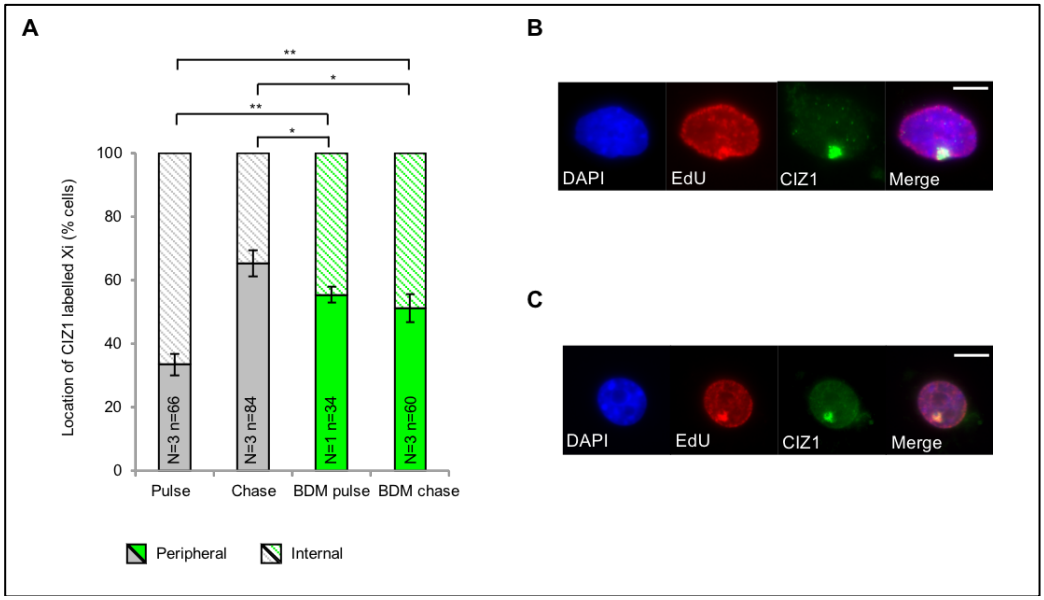

Figure 5.3. Nuclear myosin function is required for both departure and return to the nuclear periphery.

A) Mean data ±SEM for location of CIZ1-marked and EdU-labelled Xi for wild type primary embryonic fibroblasts immediately after a 30 minute pulse labelling window (grey), after a chase period (grey), immediately after a 30 minute pulse labelling window following a 30 minute incubation in the presence of BDM (green), and after a chase period in the presence of BDM (green). Average Xi departure is inhibited and average Xi return is slightly reduced, compared by students t-test. For all analysis *P≤0.05, **P≤0.01, ***P≤0.001. N=independent cell lines, n=total nuclei with replicating Xi scored. B) Representative example image of wild type primary nucleus subjected to 30 minute pulse labelling window following a 30 minute incubation in the presence of BDM, with replicating Xi, stained with EdU (red) and CIZ1 (green). DNA is blue, bar is 10 microns. C) Representative example image of wild type primary nucleus after a chase period in the presence of BDM, with replicating Xi, stained with EdU (red) and CIZ1 (green). DNA is blue, bar is 10 microns.

Ciliobrevin D was also introduced during both the EdU pulse labelling window and the chase period in order to test if dynein function was required for Xi

departure or return. No significant difference was found between the average location of CIZ1-marked EdU-labelled Xis after a 30 minute incubation with ciliobrevin D compared to the average Xi location of the pulse control (Figure 5.4A), with the majority of Xis found to be located towards the interior of the nuclei (Figure 5.4B). Conversely, there was a clear significant difference between the average location of Xis after a 30 minute chase with media containing ciliobrevin D compared to the average Xi location after the control chase (Figure 5.4A, 5.4C). The percentage of peripheral Xis decreased to 44% compared to 65% in the control chase. These results suggest dynein function is not required for Xi departure but is required for Xi return.

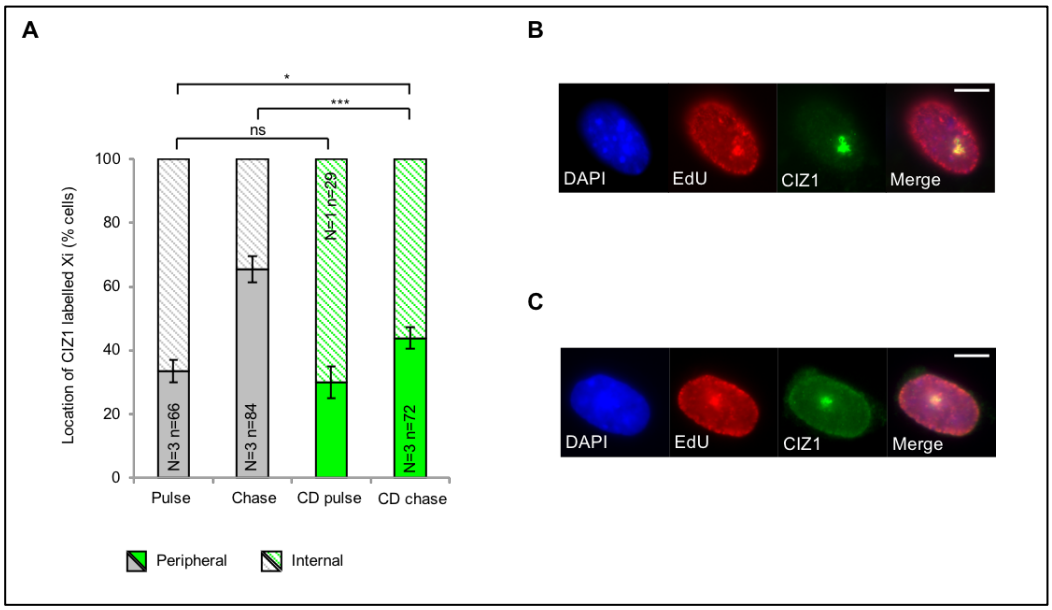

Figure 5.4. Dynein function is required for return to the nuclear periphery.
A) Mean data ±SEM for location of CIZ1-marked and EdU-labelled Xi for wild type primary embryonic fibroblasts immediately after a 30 minute pulse labelling window (grey), after a chase period (grey), immediately after a 30 minute pulse labelling window following a 30 minute incubation in the presence of Ciliobrevin D (green), and after a chase period in the presence of Ciliobrevin D (green). Average Xi departure is not inhibited and average Xi return is inhibited, compared by students t-test. For all analysis *P≤0.05, **P≤0.01, ***P≤0.001. N=independent cell lines, n=total nuclei with replicating Xi scored. B) Representative example image of wild type primary nucleus subjected to 30 minute pulse labelling window following a 30 minute incubation in the presence of Ciliobrevin D, with replicating Xi, stained with EdU (red) and CIZ1 (green). DNA is blue, bar is 10 microns. C) Representative example image of wild type primary nucleus after a chase period in the presence of Ciliobrevin D, with replicating Xi, stained with EdU (red) and CIZ1 (green). DNA is blue, bar is 10 microns.

5.4.2 Are different pathways responsible for Xi departure and return?

Interestingly, both treatment with BDM and ciliobrevin D seemed to have an inhibitory effect on Xi return, although neither produced a complete inhibitory effect. This result prompted testing of a combination of BDM and ciliobrevin D to determine whether multiple pathways were present for Xi departure and return, and whether these pathways act in a compensatory way to ensure Xi relocation still occurs to some degree. As expected, since Ciliobrevin D previously had no effect on Xi departure, results regarding the modified pulse labelling strategy

were similar to those seen after a 30 minute incubation with BDM independently, with significantly less CIZ1-marked EdU-labelled Xis located at the nuclear interior. The percentage of internal Xis decreased to 40% following a 30 minute incubation with the combination compared to 67% in the pulse control (Figure 5.5A, 5.5B). The main reasoning behind the combination concerned Xi return. With regard to the modified chase strategy, there was a clear significant difference between the Xi location after a 30 minute chase with media containing the combination compared to the average Xi location after the control chase (Figure 5.5A, 5.5C), with the percentage of peripheral Xis decreasing to 30% compared to 65% in the control chase. This result closely mimicked that of the control pulse, unlike the application of the treatments independently, suggesting complete inhibition was achieved.

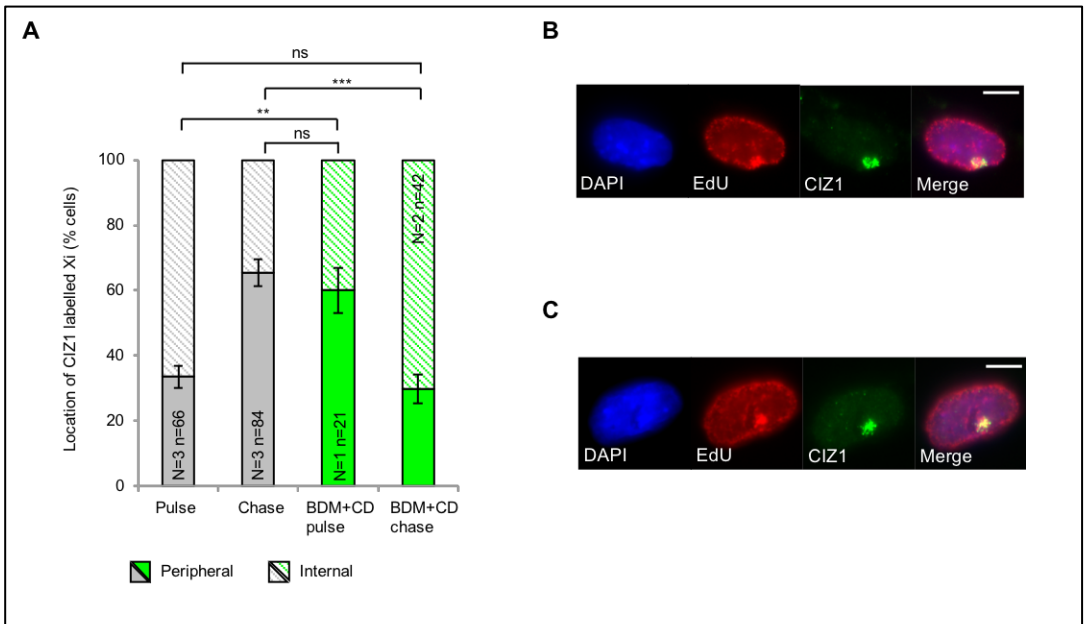

Figure 5.5. Multiple pathways are responsible for return to the nuclear periphery. A) Mean data ±SEM for location of CIZ1-marked and EdU-labelled Xi for wild type primary embryonic fibroblasts immediately after a 30 minute pulse labelling window (grey), after a chase period (grey), immediately after a 30 minute pulse labelling window following a 30 minute incubation in the presence of a combination of BDM and Ciliobrevin D (green), and after a chase period in the presence of a combination of BDM and Ciliobrevin D (green). Average Xi departure is inhibited and average Xi return is inhibited, compared by students t-test. For all analysis *P≤0.05, **P≤0.01, ***P≤0.001. N=independent cell lines, n=total nuclei with replicating Xi scored. B) Representative example image of wild type primary nucleus subjected to 30 minute pulse labelling window following a 30 minute incubation in the presence of a combination of BDM and Ciliobrevin D, with replicating Xi, stained with EdU (red) and CIZ1 (green). DNA is blue, bar is 10 microns. C) Representative example image of wild type primary nucleus after a chase period in the presence of a combination of BDM and Ciliobrevin D, with replicating Xi, stained with EdU (red) and CIZ1 (green). DNA is blue, bar is 10 microns.

5.5 Discussion

5.5.1 Interpreting the mechanisms of Xi departure and return

Uncovering mechanistic information and the requirements of Xi relocation was the primary target from the start. This will hopefully act as the first steps in characterizing the requirements of something very new and clinically relevant. Experiments in this chapter have identified one possible pathway responsible for Xi departure, although there is speculation surrounding a second pathway, and two possible pathways responsible for Xi return. When looking at Xi departure, BDM was the only inhibitor seen to have an inhibitory effect. This result was supported by the combination of BDM and ciliobrevin D producing a very similar effect as BDM independently, suggesting that Xi departure requires nuclear myosin function. Interestingly, inhibition with BDM did not produce a complete inhibitory effect on Xi departure, suggesting there may be another unknown component required. Moving on to Xi return, as mentioned above, both BDM and ciliobrevin D had an inhibitory effect, although neither seemed to produce full inhibition. Washout with the combination of BDM and ciliobrevin D produced results very similar to those of the control pulse, with 70% of Xis being located towards the nuclear interior. This suggests that full inhibition of Xi return has taken place, and therefore, also suggests that Xi return requires nuclear myosin function and dynein function only. Seeing as BDM and ciliobrevin D did not produce complete inhibition independently, it is plausible that nuclear myosin and dynein act in compensation, meaning blockage of one pathway will result in the other taking over to ensure Xi return still occurs, albeit not with the optimum efficiency.

In addition, it seems that inhibition of dynein produced a greater effect on Xi return than inhibition of nuclear myosin. This implies that dynein is the primary mechanism for Xi return, with nuclear myosin acting as a facilitative backup. However, further experimentation, most likely consisting of increasing the concentration of BDM and ciliobrevin D, is required to confirm this hypothesis.

As previously mentioned, it seems another component is involved in Xi departure alongside nuclear myosin, as BDM did not produce a full inhibitory effect (Figure

5.3A). However, even with the combination of BDM and Ciliobrevin D having a similar effect on the percentage of internally located Xi's to inhibition with BDM independently, results imply that the combination produced complete inhibition of Xi departure (Figure 5.5A). Nevertheless, in both cases only one independent cell line was tested. Therefore, immediate experimentation of the three wild type primary cell lines (with technical replicates) used throughout is required to expand on this observation before a conclusion can be reached. Interestingly, although it was not possible to test if ongoing DNA synthesis was required for Xi departure, inhibition with aphidicolin seemed to produce a slight increase in the percentage of cells with an Xi located at the nuclear periphery when testing requirements for Xi return (Figure 5.2C). This observation leads to the suggestion that ongoing DNA synthesis may in fact be required for Xi departure and may be the unknown component alluded to earlier. This suggestion is entirely hypothetical at this stage, requiring development of an alternative assay, which will allow testing of DNA synthesis in Xi departure.

A possibility that should be acknowledged concerns an increase in the speed of Xi relocation mechanism as a result of inhibition. For example, the blockage of Xi departure by BDM may be causing an increase in Xi movement speed, not inhibition of departure. If this were true, the Xi would have migrated inward, progressed through replication and returned to the periphery within the 30 minute pulse labelling period. This would result in a higher percentage of peripheral Xis, as seen upon inhibition with BDM. A pulse labelling time course, consisting of labelling windows of 5 and 10 minutes, would test this possible alternative explanation.

These results and hypotheses allow the initial formulation of a model that describes the mechanisms by which Xi relocation takes place (Figure 5.6), with the Xi moving towards the nuclear interior via nuclear myosin and subsequently returning to the periphery via a combination of dynein and nuclear myosin after DNA synthesis. Notably, Ciliobrevin D is described as a cytoplasmic dynein inhibitor. Since Xi relocation occurs within the nucleus, and Ciliobrevin D has an inhibitory effect on Xi return, it is logical to suggest that Ciliobrevin D inhibits nuclear dynein. Although, to my knowledge, there is no direct evidence for dynein function within the nucleus. It is important to be open-minded when interpreting

results, therefore it is possible that Xi return requires nuclear dynein function (Figure 5.6A) or requires external input of cytoplasmic dynein to pull the Xi to the periphery (Figure 5.6B). One method to experimentally distinguish whether Xi return is carried out by nuclear or cytoplasmic dynein function could be by combining polarized total internal reflection (polTIRF) microscopy and high precision localisation to track the position and orientation of dynein molecules in real time (Lippert et al. 2015), although currently no discussion has occurred regarding this.

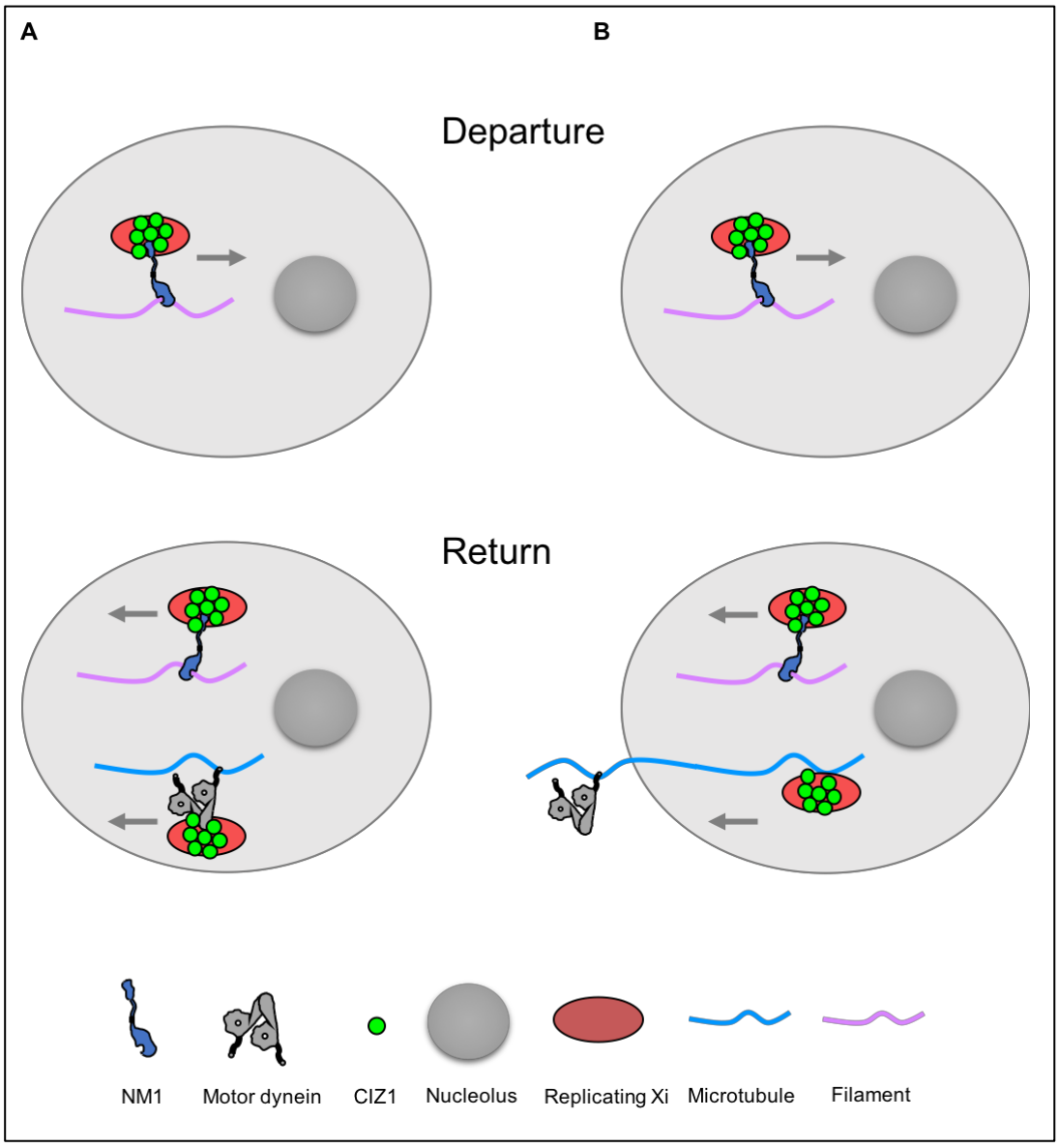

Figure 5.6. Summary interpretation of mechanism of Xi departure and return to periphery.

Model proposes two alternatives for Xi relocation. A) Departure of CIZ1-Xi towards the nuclear interior occurs via nuclear myosin 1 and return occurs via a facilitative combination of nuclear myosin and nuclear dynein (left). B) Departure of CIZ1-Xi towards the nuclear interior occurs via nuclear myosin 1 and return occurs via a facilitative combination of nuclear myosin and cytoplasmic dynein (right).

Chapter 6. Development of an alternative assay: Thymidine arrest

6.1 Introduction

Up to this point, all data concerning movement of the Xi was produced using incorporation of EdU during a labelling window. This method allowed clear visual indication of cells that were naturally cycling and progressing through S phase, making scoring easy. Furthermore, results were reproducible, as shown, making EdU incorporation a valuable technique for characterising Xi relocation. However, extensive testing using the method highlighted multiple disadvantages. In general, a single coverslip contained around 1000 cells. Of those, approximately 30% were progressing through S phase, therefore would incorporate EdU. Approximately 10% of those cells progressing through S phase had a detectable replicating Xi, meaning only around 3% of cells on a coverslip were scorable. Consequently, production of a complete data set was both labour intensive and time consuming. The protocol itself was also very time consuming, often taking a full day to complete. In addition, the low frequency makes the protocol incompatible with biochemical analysis, which would aid in uncovering crucial aspects of the mechanism. For these reasons, development of an alternative assay was desirable. Thymidine is a pyrimidine nucleoside capable of interrupting the deoxynucleotide metabolism pathway, halting dCTP synthesis and therefore DNA replication (Morris et al. 1963) resulting in an early S phase blockade. Since Xi movement occurs in S phase it was suggested that arrest using thymidine might trap cells during the movement window, allowing much easier analysis of movement characteristics and requirements owing to a greater proportion of cells being engaged in the events under investigation.

6.2 Aims

The aim of the work described in this chapter was to develop:

i) an alternative assay utilizing thymidine arrest to evaluate the location and area of CIZ1-marked Xi in all cells.
ii) a strategy to evaluate the requirements of Xi relocation utilizing thymidine arrest, testing inhibition of specific pathways of interest that have been mentioned previously.

6.3 Experimental Procedure

Thymidine was used to arrest cells in early S phase (Methods 2.2.3; Figure 6.1A) allowing visualisation of CIZ1-marked Xis in the arrested state, and comparison with a synchronised cycling population following arrest with and washout of thymidine (Figure 6.1B). Xi location was scored, and area quantified. Co-staining with anti-H2AK119Ub1 was used as Xi confirmation (Figure 6.1C). An imageJ macro, entitled “Area.macro”, was written for automated processing of images to produce area information (Methods 2.6; Figure 6.1D).

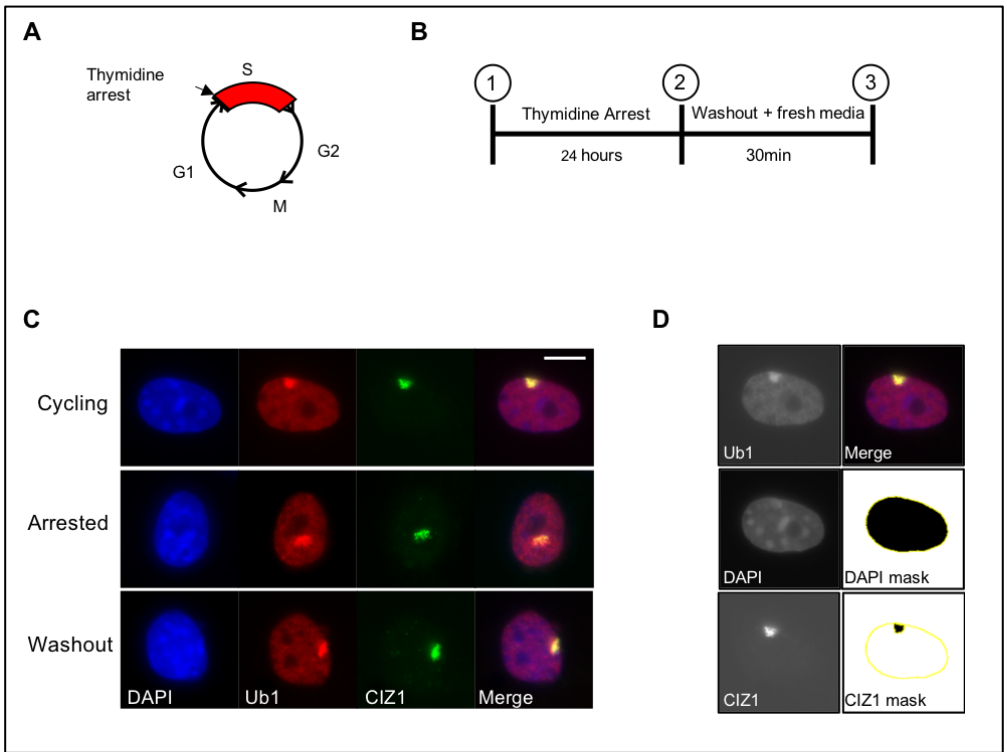

Figure 6.1. Alternative assay development: evaluation of CIZ1-marked Xi in all cells. A) Schematic representation of the cell cycle showing incorporation of the pyrimidine nucleoside thymidine, gradually arresting cells in early S phase. B) Timeline of thymidine arrest protocol, with sampling at time points 1 (before), 2 (after) and 3 (after a washout of thymidine and return to cycle). C) Example images of wild type primary nuclei stained for H2AK119Ub1 (red) and CIZ1 (green) showing Xis from time points 1, 2 and 3 (cycling, arrested and washout). DNA is blue, bar is 10 microns. D) Evaluation of area occupied: example images produced during area quantification using ImageJ to measure extent of CIZ1 and Xi dispersal. H2AK119Ub1 (top left), DNA (middle left), DNA area mask (middle right), CIZ1 (bottom left), CIZ1 area mask (bottom right).

Modification of the thymidine arrest protocol allowed development of a strategy to test Xi relocation requirements. Modification involved a 24 hour arrest with thymidine and the inhibitor to test requirements of Xi departure (Figure 6.2, pathway 1), or a 30 minute washout with media containing the inhibitor after arresting with thymidine to test requirements of Xi return (Figure 6.2, pathway 2).

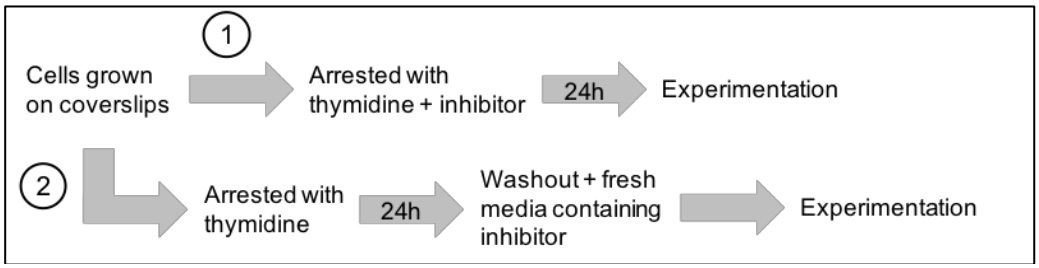

Figure 6.2. Strategy for evaluation of the requirements of Xi relocation using thymidine arrest.
Timeline for modification of thymidine arrest protocol allowing evaluation of requirements for Xi departure (pathway 1) and Xi return (pathway 2).

6.4 Results

6.4.1 Assay development

Before full development of the assay could begin, testing the ability of thymidine to block cells in S phase was required. Two independent populations of primary embryonic fibroblasts (E13.8) were grown on separate plates (Methods 2.1.4). One plate was kept as the cycling control while the other was incubated in media containing thymidine for 24 hours. Samples were taken from both plates and analysed via flow cytometry. The sample from the plate treated with thymidine produced a curve indicative of accumulation of cells in S phase while the control curve showed a regular cell cycle profile with both G1 and G2 peaks, confirming thymidine activity (Figure 6.3A).

It was then possible to determine whether Xi movement could be seen using thymidine arrest. As in the tests with EdU, three populations of primary cells isolated from independent wild type embryos (E14.4, E13.1 and E13.8) were used. As expected, in the cycling populations, CIZ1-marked Xis were

predominately found to be located at the periphery of the nuclei, with 81% of Xis being scored as peripheral. Following a 24 hour thymidine arrest, 58% of Xis were still found to be located at the periphery, but there was a clear significant increase in the number of internal Xis, with 24% more of the population being scored as internal. Finally, following a washout, results were very similar to those of the cycling population, with 76% of Xis being located at the nuclear periphery. These results were seen in all three independent primary populations, each of which had three technical replicates scoring 50 nuclei per replicate (Figure 6.3B). Interestingly, following thymidine arrest, inward movement of CIZ1 was accompanied by the inward movement of enriched H2AK119Ub1.

In addition to information regarding Xi location within the nuclei, thymidine arrest also allowed information regarding Xi area to be produced. As previously explained (Methods 2.6), area measurements for CIZ1-marked Xis and DAPI-stained nuclei from imageJ were used to calculate the percentage area of the nucleus occupied by CIZ1. Testing consisted of 20 images per condition with three technical replicates per cell line (E13.1, E13.8, E14.4). After arrest with thymidine, the area within the nuclei occupied by CIZ1 was significantly greater compared to the cycling populations. Moreover, the area increase was reversed following the washout (Figure 6.3C).

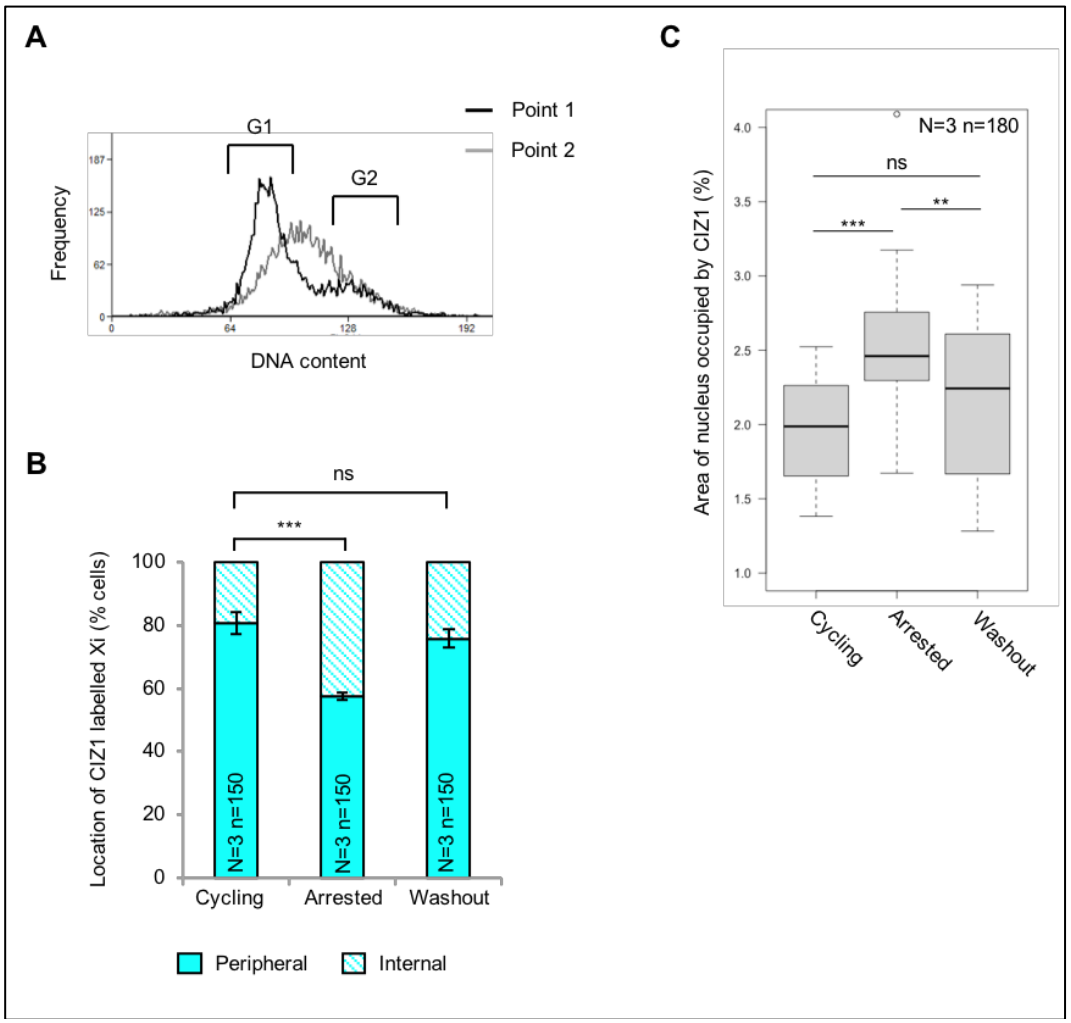

Figure 6.3. Evaluation of the location and area of CIZ1-Xi in wild type primary cells. A) Flow cytometry profiles of populations isolated at points 1 and 2 (Figure 6.1B), to verify the effect of thymidine on cell cycle progression. Cells were stained with propidium iodide to reveal DNA content with help from staff of York Bioscience Technology facility. B) Evaluation of location: mean data ±SEM for location of CIZ1-labelled Xi for three wild type primary embryonic fibroblasts (E14.4, E13.8, E13.1) at time points 1, 2 and 3 (Figure 6.1B). Xi shifts location following arrest via thymidine and returns following the washout, compared by students t-test. *P≤0.05, **P≤0.01, ***P≤0.001. N=independent cell lines, n=total nuclei scored. C) Box plot showing percentage area of nucleus occupied by CIZ1 for three wild type primary embryonic fibroblasts (E14.4, E13.8, E13.1) rapidly cycling (n=20, median=1.99, range=1.38-2.52), compared to arrest via thymidine (n=20, median=2.46, range=1.67-4.09), compared to after a washout and fresh media (n=20, median=2.24, range=1.28-2.94).

6.4.2 Utilizing thymidine arrest to determine the requirements of Xi relocation

With a suspected working alternative assay to study Xi relocation, the next step was to utilize the assay to determine the requirements of Xi departure and return, as well as monitoring any changes in CIZ1-marked Xi area, to reveal further important mechanistic information.

Unlike EdU incorporation, thymidine arrest allowed proposition of the question “is ongoing DNA synthesis required for Xi departure?”. Three populations of primary cells isolated from independent wild type embryos (E13.1, E13.8, E14.4) underwent modified thymidine arrest with the addition of aphidicolin (DNA polymerase α inhibitor), BDM (nuclear myosin inhibitor), ciliobrevin D (cytoplasmic dynein inhibitor) and a combination of BDM and ciliobrevin D. With regard to treatment with aphidicolin, 83% of CIZ1-marked Xi were found to be located at the nuclear periphery following a 24 hour thymidine arrest with the addition of aphidicolin (Figure 6.4A). This result mimicked what was seen in the cycling populations, appearing to block the action of thymidine. CIZ1-marked Xis were also found to be smaller in relative area than arrested Xis, again being more similar to that of the cycling populations (Figure 6.4B, 6.4C). In addition, there was no significant difference between the average Xi location after a washout with media containing aphidicolin compared to the control washout with fresh media, with Xi returning to the nuclear periphery in both cases (Figure 6.1A). There was also no significant difference in the average relative area occupied by CIZ1-marked Xis after a washout with media containing aphidicolin compared to the control washout with fresh media (Figure 6.4B, 6.4D). These results suggest that blocking ongoing DNA synthesis during early S phase before the Xi has replicated prevents both internalisation and expansion of the Xi, however, the treatment does not prevent subsequent return to the periphery and condensation after Xi replication.

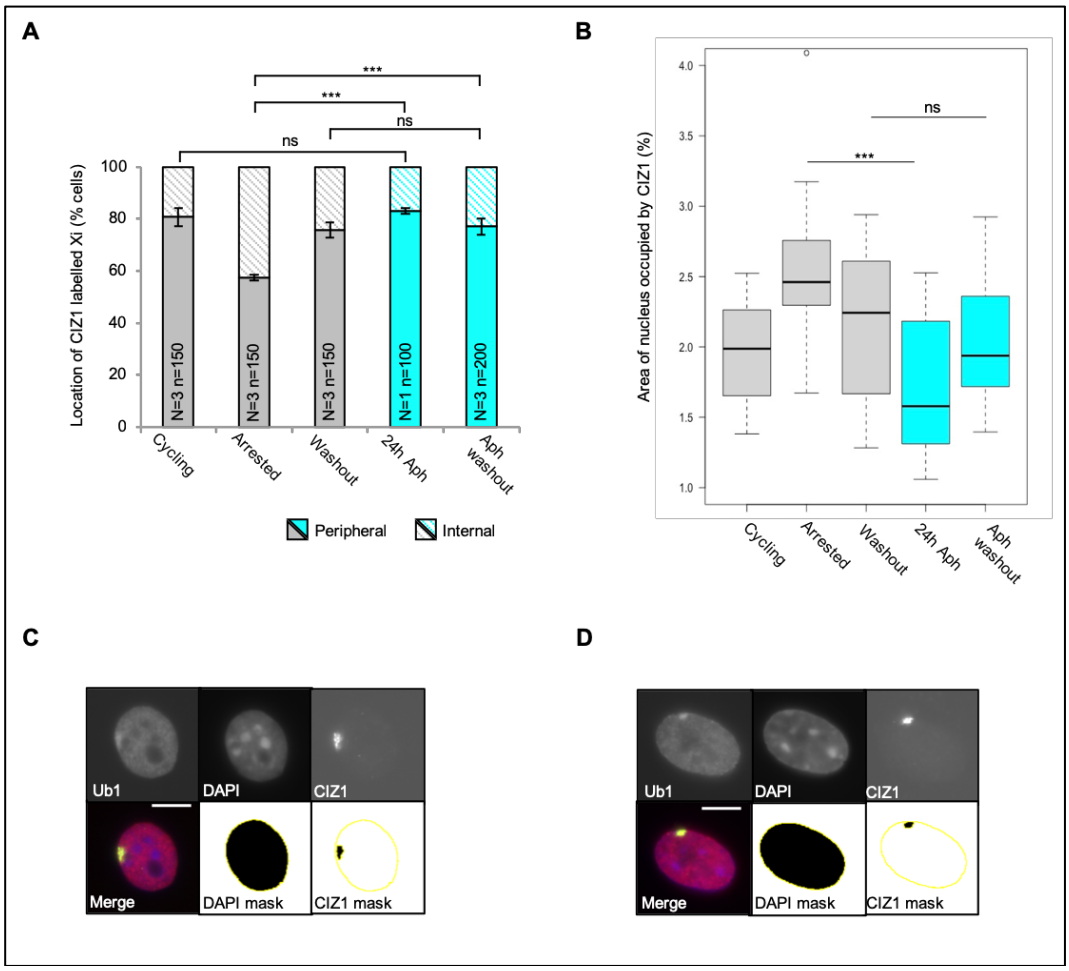

Figure 6.4. Evaluation of location and area following inhibition with Aphidicolin. A) Mean data ±SEM for location of CIZ1-marked Xi for wild type primary embryonic fibroblasts at time points 1, 2 and 3 (Figure 6.1B, grey), arrested via thymidine with Aphidicolin (blue), and after a washout and fresh media with Aphidicolin (blue). Accumulation of cells in which CIZ1-marked Xi is located internally is reduced following arrest with Aphidicolin and Xi position is no different following washout with Aphidicolin, compared by students t-test. B) Box plot showing percentage area of nucleus occupied by CIZ1 for wild type primary embryonic fibroblasts at time points 1, 2 (n=20, median=2.46, range=1.67-3.17) and 3 (n=20, median=2.24, range=1.28-2.94), arrested via thymidine with Aphidicolin (n=20, median=1.58, range=1.06-2.53), and after a washout and fresh media with Aphidicolin (n=20, median=1.94, range=1.40-2.92). For all analysis *P≤0.05, **P≤0.01, ***P≤0.001. N=independent cell lines, n=total nuclei scored. C) Example images of wild type primary nucleus arrested via thymidine with Aphidicolin produced during area quantification as in Figure 6.1D. D) Example images of wild type primary nucleus after a washout and fresh media with Aphidicolin produced during area quantification as in Figure 6.1D. Bar is 10 microns.

With regard to BDM, the percentage of CIZ1-marked Xis located internally was slightly reduced, with 35% of Xis being scored as internal following a 24 hour thymidine arrest with the addition of BDM compared to 43% in the control thymidine arrest (Figure 6.5A). Interestingly, there was no significant difference between the average relative area of CIZ1-marked Xis following a 24 hour thymidine arrest with BDM compared to the control (Figure 6.5B, 6.5C). Following the washout with media containing BDM, the percentage of Xis located peripherally was significantly less than that seen following the control washout with fresh media, 61% and 76% internal respectively (Figure 6.2A). As well as this, the average relative size of CIZ1-marked Xis after a washout with media containing BDM was also significantly greater than that seen following a control washout with fresh media (Figure 6.5B, 6.5D). These results suggest that blocking nuclear myosin function before Xi replication prevents internalisation but not expansion of the Xi. In addition, blocking nuclear myosin function after Xi replication prevents return and condensation of the Xi.

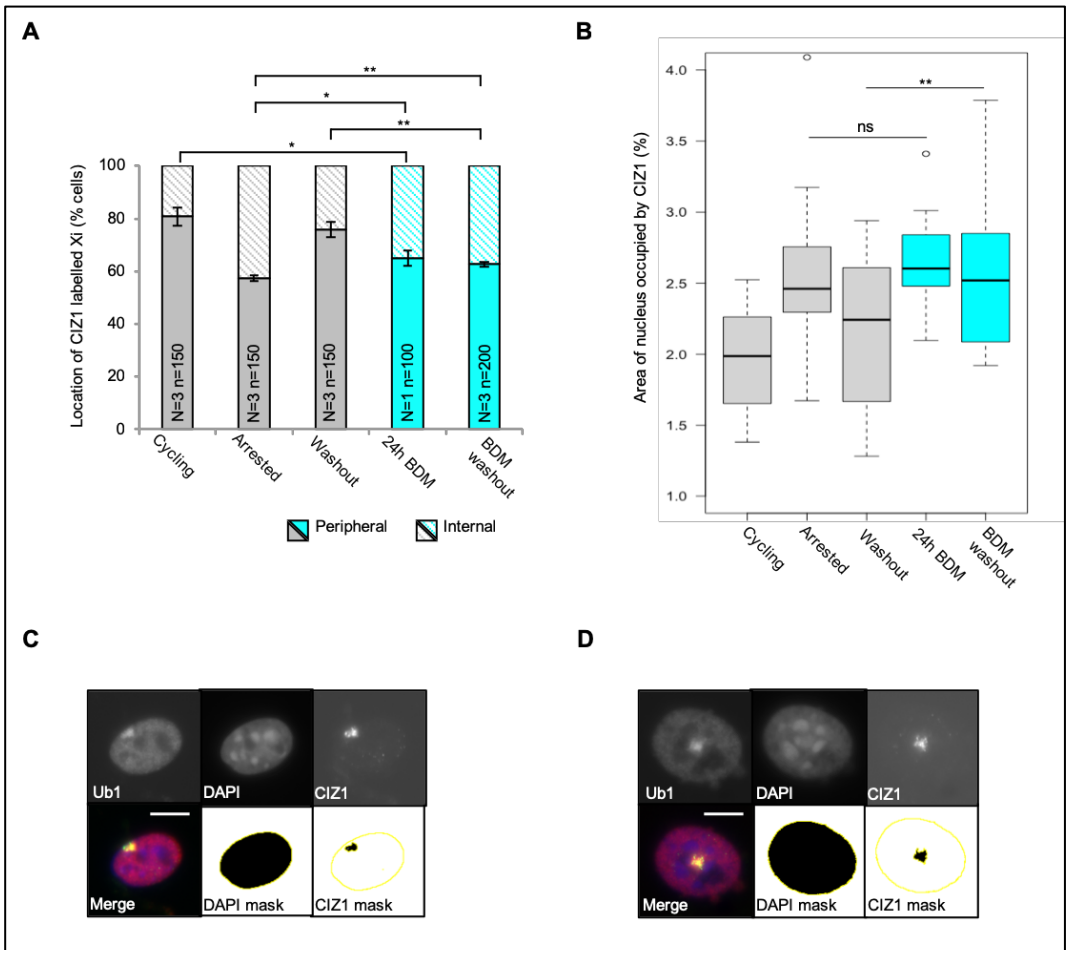

Figure 6.5. Evaluation of location and area following inhibition with BDM.
A) Mean data ±SEM for location of CIZ1-marked Xi for wild type primary embryonic fibroblasts at time points 1, 2 and 3 (Figure 6.1B, grey), arrested via thymidine with BDM (blue), and after a washout and fresh media with BDM (blue). Accumulation of cells in which CIZ1-marked Xi is located internally is slightly reduced following arrest with BDM and accumulation of cells in which CIZ1-marked Xi is located peripherally is reduced following washout with BDM, compared by students t-test. B) Box plot showing percentage area of nucleus occupied by CIZ1 for wild type primary embryonic fibroblasts at time points 1, 2 (n=20, median=2.46, range=1.67-3.17) and 3 (n=20, median=2.24, range=1.28-2.94), arrested via thymidine with BDM (n=20, median=2.60, range=2.10-4.80), and after a washout and fresh media with BDM (n=20, median=2.52, range=1.92-3.79). For all analysis *P≤0.05, **P≤0.01, ***P≤0.001. N=independent cell lines, n=total nuclei scored. C) Example images of wild type primary nucleus arrested via thymidine with BDM produced during area quantification as in Figure 6.1D. D) Example images of wild type primary nucleus after a washout and fresh media with BDM produced during area quantification as in Figure 6.1D. Bar is 10 microns.

Due to time constraint, Ciliobrevin D was only tested in the washout. The percentage of CIZ1-marked Xis located peripherally significantly decreased, with 62% of cells having a peripheral Xi compared to 76% following the control washout with fresh media (Figure 6.6A). In addition, the average relative area occupied by CIZ1-marked Xis also increased compared to the control washout (Figure 6.6B, 6.6C). These results suggest that blocking dynein function after Xi replication prevents return and condensation of the Xi.

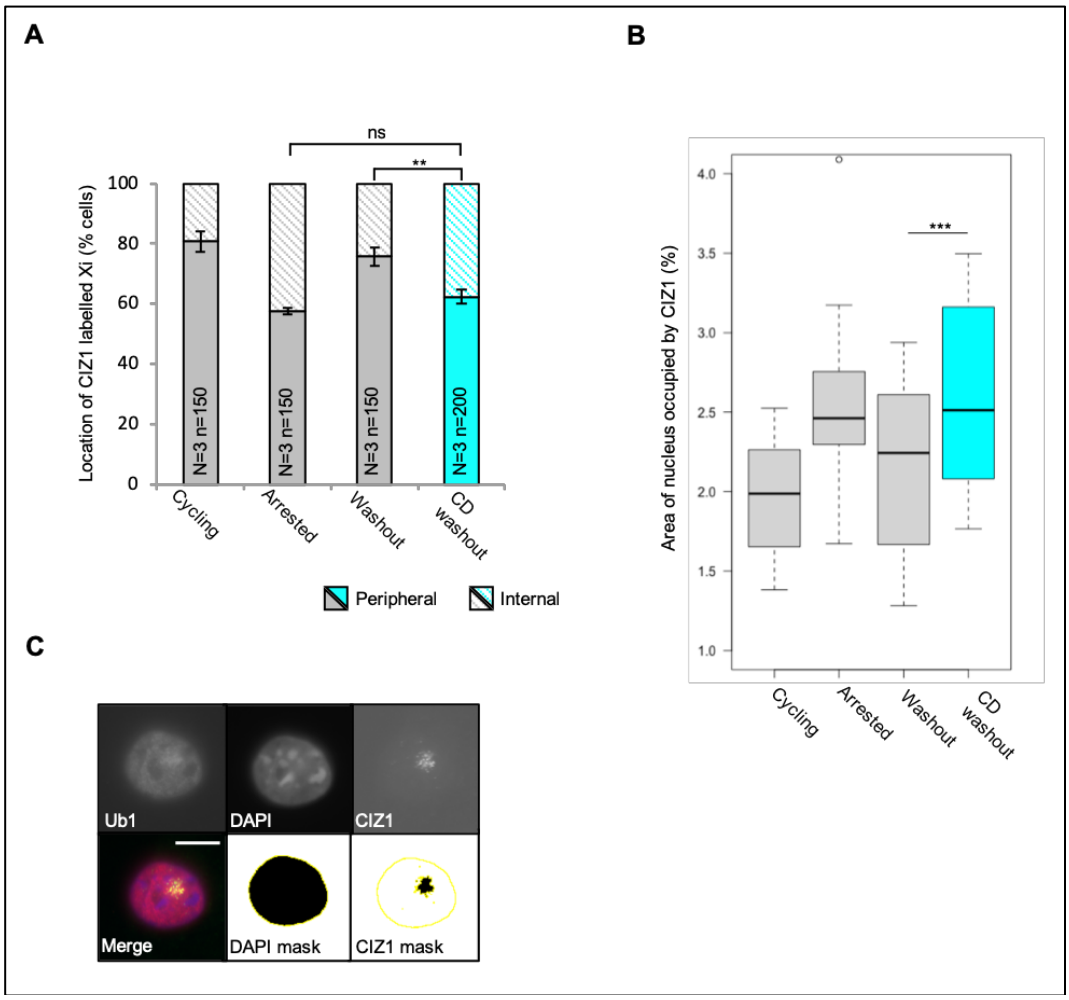

Figure 6.6. Evaluation of location and area following inhibition with Ciliobrevin D. A) Mean data ±SEM for location of CIZ1-marked Xi for wild type primary embryonic fibroblasts at time points 1, 2 and 3 (Figure 6.1B, grey), and after a washout and fresh media with Ciliobrevin D (blue). Accumulation of cells in which CIZ1-marked Xi is located peripherally is reduced, compared by students t-test. B) Box plot showing percentage area of nucleus occupied by CIZ1 for wild type primary embryonic fibroblasts at time points 1, 2 (n=20, median=2.46, range=1.67-3.17) and 3 (n=20, median=2.24, range=1.28-2.94), and after a washout and fresh media with Ciliobrevin D (n=20, median=2.51, range=1.77-3.50). For all analysis *P≤0.05, **P≤0.01, ***P≤0.001. N=independent cell lines, n=total nuclei scored. C) Example images of wild type primary nucleus after a washout and fresh media with Ciliobrevin D produced during area quantification as in Figure 6.1D. Bar is 10 microns.

Replicating what was seen via EdU incorporation, both BDM and CD were seen to have an inhibitory effect on Xi return. However, results from the thymidine arrest assay suggest that Ciliobrevin D completely inhibits Xi return (Figure 6.6A), whereas BDM does not completely inhibit return (Figure 6.5A), differing from what was seen via EdU incorporation. Nonetheless, the combination of BDM and Ciliobrevin D was tested via thymidine arrest. As expected, the percentage of CIZ1-marked Xis located peripherally significantly decreased following a washout with media containing the combination, with 60% of cells having a peripheral Xi compared to 76% following the control washout with fresh media (Figure 6.7A). Interestingly, this was a greater increase than was found following inhibition with BDM and ciliobrevin D independently. Furthermore, the average relative area occupied by CIZ1-marked Xis following the washout with media containing the combination was significantly greater than that seen in the control washout (Figure 6.7B, 6.7C), similar to what was found following treatment with BDM and ciliobrevin D independently. These results suggest that blocking both dynein and nuclear myosin at the same time after Xi replication completely prevents Xi return and prevents condensation of the Xi.

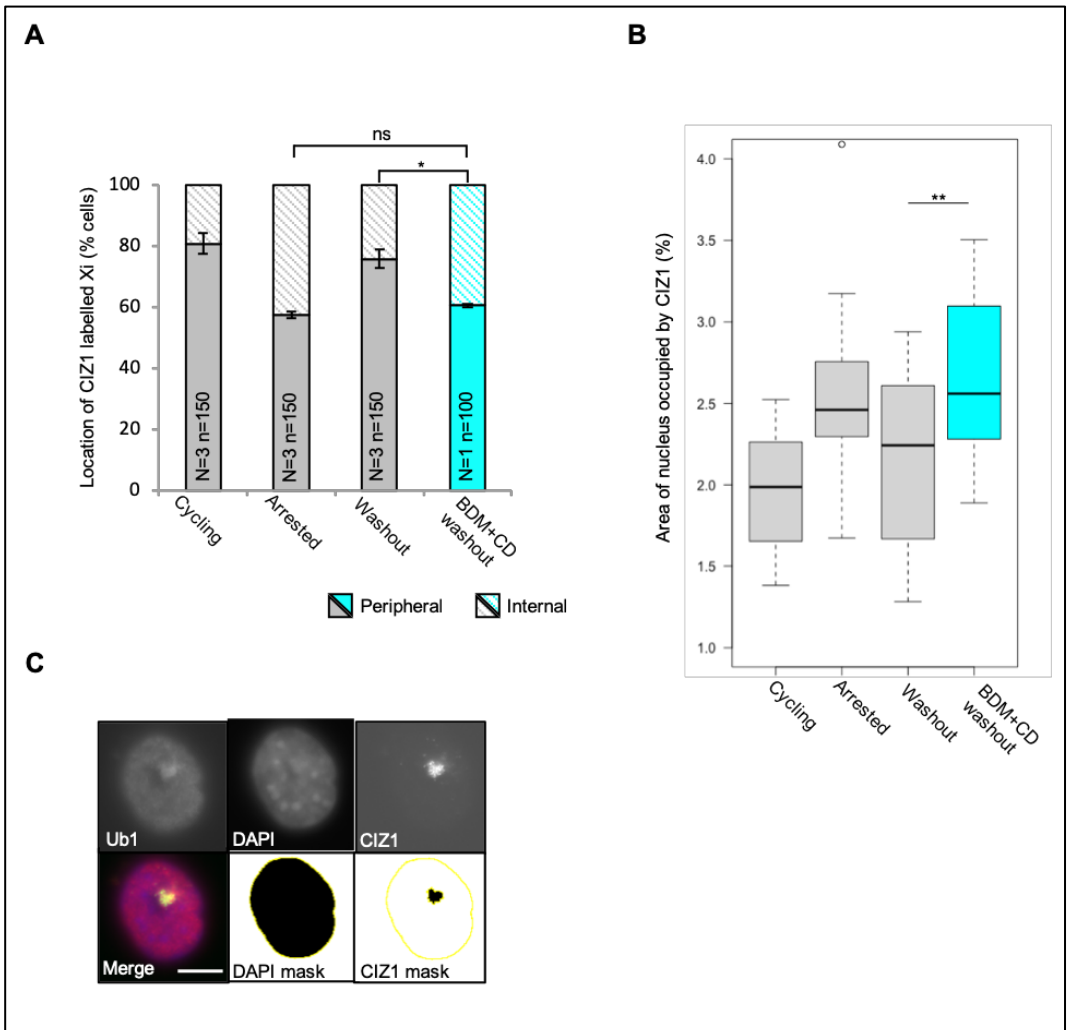

Figure 6.7. Evaluation of location and area following inhibition with a combination of BDM and Ciliobrevin D.

A) Mean data ±SEM for location of CIZ1-marked Xi for wild type primary embryonic fibroblasts at time points 1, 2 and 3 (Figure 6.1B, grey), and after a washout and fresh media with combination of BDM and Ciliobrevin D (blue). Accumulation of cells in which CIZ1-marked Xi is located peripherally is reduced, compared by students t-test. B) Box plot showing percentage area of nucleus occupied by CIZ1 for wild type primary embryonic fibroblasts at time points 1, 2 (n=20, median=2.46, range=1.67-3.17) and 3 (n=20, median=2.24, range=1.28-2.94), and after a washout and fresh media with combination of BDM and Ciliobrevin D (n=20, median=2.51, range=1.77-3.50). For all analysis *P≤0.05, **P≤0.01, ***P≤0.001. N=independent cell lines, n=total nuclei scored. C) Example images of wild type primary nucleus after a washout and fresh media with combination of BDM and Ciliobrevin D produced during area quantification as in Figure 6.1D. Bar is 10 microns.

6.5 Discussion

It became apparent that development of an alternative to EdU incorporation was key to fully understand and reveal the mechanisms used by the Xi for movement. Thymidine arrest combats the shortcomings of EdU incorporation by allowing all cells on a coverslip to be detected and therefore scorable, as well as being compatible for biochemical analysis. Moreover, without the need of a pulse labelling window and a chase period, thymidine arrest is the quicker of the two assays following planning in advance. Importantly, outputs from both the EdU incorporation and thymidine arrest were the same, showing Xi departure and return, confirming that thymidine arrest was a viable alternative assay for future progression. Although the output trends are the same, the results of thymidine arrest are less striking. The difference in location of CIZ1-marked Xis after thymidine arrest compared to the cycling populations could be classed as minimal, with only a 20% increase in the percentage of internal Xis. However, statistical analysis suggests that this small difference is very significant, mainly due to the high reproducibility of the result, further supporting the idea that thymidine arrest is a viable alternative. The reason for only a small increase in the percentage of internal Xis following thymidine arrest is unknown. It is possible that a proportion of the cells used for the experiment had not re-entered the cell cycle after thawing, and so had not stopped in S phase. This analysis uses early passage cells of limited availability, so they were not subject to multiple cycles prior to analysis. Since CIZ1 appears to co-localise with the Xi chromatin as CIZ1 moves inward (shown by CIZ1 and H2AK119Ub1 co-localisation following thymidine arrest) evaluation of Xi location in CIZ1 null primary populations would act as an additional control to further support the use of thymidine arrest.

Progressing onto application of inhibitors. Similar to what was seen via EdU incorporation, BDM had a slight inhibitory effect on Xi departure. As alluded to previously, it was hypothesised that DNA synthesis was also required for Xi departure, as BDM did not produce a full inhibitory effect. The thymidine arrest assay is compatible with the addition of aphidicolin to test this hypothesis. Interestingly, aphidicolin also seemed to block the effects of thymidine on the Xi, completely inhibiting departure. This suggests that Xi departure requires ongoing DNA synthesis and nuclear myosin function. We hypothesize that the incomplete

inhibition of DNA synthesis achieved with thymidine is not sufficient to impact Xi internalization. Again, as was seen via EdU incorporation, both BDM and ciliobrevin D had an inhibitory effect on Xi return, with the percentage of internal Xis increasing. However, washing with fresh media and Ciliobrevin D produced full inhibition of return, differing to what was seen via EdU. Interestingly, via EdU incorporation, inhibition of dynein produced a greater effect on Xi return than inhibition of nuclear myosin. Results here reinforce the suggestion that dynein is involved in the primary mechanism for Xi return, with the nuclear myosin pathway acting as a facilitative backup. As expected, washout with media containing the combination of BDM and ciliobrevin D resulted in greater percentage of internal Xis than the treatments independently. Statistically, the increase in internal Xis produced by the combination was less significant than that produced by BDM and ciliobrevin D independently. Small N and n numbers are likely responsible, meaning it would be plausible to expect the significance of the combination to increase upon further testing.

Unique to the thymidine arrest assay was CIZ1-marked Xi area measurements, adding another aspect of analysis to the developing story. The percentage area of the nucleus occupied by CIZ1 significantly increased following arrest with thymidine. This increase then appeared to be reversed following the washout. The cause and implication of the area increase upon arrest is currently unknown. It is possible that it is physiologically relevant, implying dispersal is part of the mechanism of Xi movement or to facilitate replication. Conversely, the increase may signify nuclei being held in one state for too long, leading to diffusion, having nothing to do with Xi movement. It is possible that a shorter, double thymidine block (Ma and Poon 2011) would still arrest cells in S phase as well as minimising the time spent arrested. In addition, a double thymidine block would increase the percentage of cells arrested in S phase. In spite of this, thymidine-induced cytotoxicity, such as failure to recover and apoptosis, are often associated with a double thymidine block (Fried et al. 1981).

If Xi area is linked to Xi movement, one would expect an inhibitor that blocks Xi departure to also produce a decrease in CIZ1-marked Xi size and an inhibitor that blocks Xi return to also produce an increase in CIZ1-marked Xi size. During Xi departure, aphidicolin produced a decrease in Xi size, true to the suggested

hypothesis. Unexpectedly, even though BDM counteracted the effect of thymidine arrest on internalization, there was no significant change in the percentage area of the nucleus occupied by CIZ1. With regard to Xi return, BDM, ciliobrevin D and the combination all resulted in a significant increase in CIZ1-marked Xi area compared to controls, again supporting the suggested hypothesis. Due to time constraints, only around 20 images per population were used to calculate area measurements. In addition, for experiments concerning Xi departure and the combination of BDM and Ciliobrevin D on Xi return, the N and n numbers were small, possibly leading to overinterpretation. Although results for most of these are promising and do appear to fit the hypothesis, it is possible that both these reasons are responsible for the insignificant CIZ1-marked Xi area following BDM arrest. Given more time, it would be of use to again expand analysis to the three primary wild type populations (E13.1, E13.8, E14.4), that have been routinely tested throughout this study, with at least three technical replicates per cell line. Furthermore, confirmation of ciliobrevin D having no effect on CIZ1-marked Xi area prior to Xi replication and the combination of BDM and Ciliobrevin D having a significant effect would act as useful support and should be looked at in the future.

Results in this chapter have not only supported the previous model but have also allowed additions to be made in order to produce an updated hypothetical model (Figure 6.8). The model interpreting the mechanism by which Xi movement occurs suggests two possible alternatives. The Xi moves towards the nuclear interior via nuclear myosin-based pathways, requiring ongoing DNA synthesis, and returns to the nuclear periphery after DNA replication via nuclear dynein-based (Figure 6.8A), or cytoplasmic dynein-based pathways (Figure 6.8B) and nuclear myosin. The departure is accompanied by the dispersal of Xi chromatin, which is reversed once DNA replication has been completed. As previously stated, this is hypothetical at this point in time, with interpretations open for debate until rigorously tested. Plans to test the hypothesis are currently being developed.

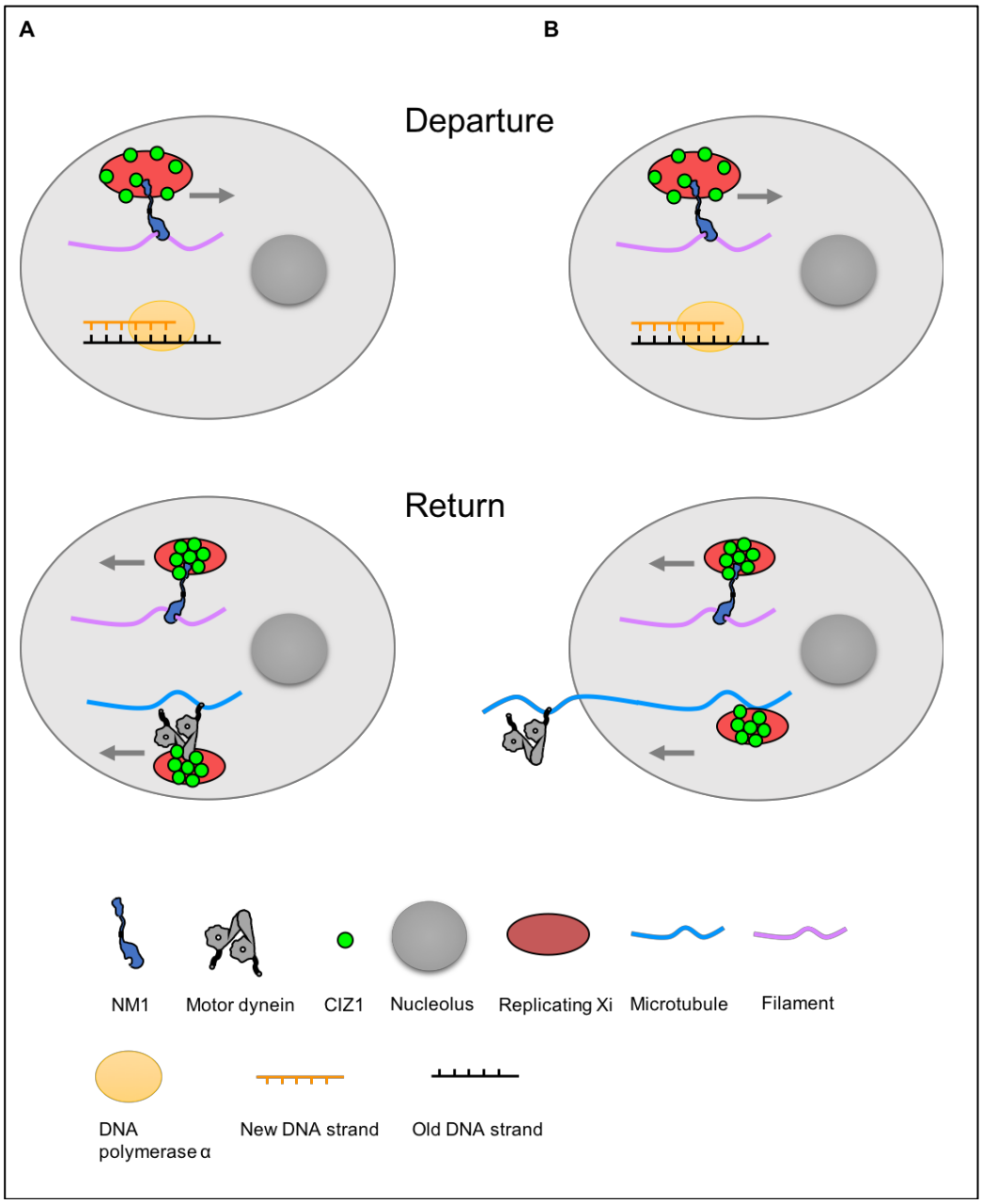

Figure 6.8. Updated summary interpretation of mechanism of Xi departure and return to periphery with CIZ1-Xi dispersal.

Model proposes two alternatives for Xi relocation. A) Departure of CIZ1-Xi towards the nuclear interior occurs via nuclear myosin 1 and return occurs via a facilitative combination of nuclear myosin and nuclear dynein (left). B) Departure of CIZ1-Xi towards the nuclear interior occurs via nuclear myosin 1 and return occurs via a facilitative combination of nuclear myosin and cytoplasmic dynein (right). In both cases, departure is accompanied by the dispersal of Xi chromatin, which is reversed once DNA replication has been completed.

Chapter 7. Discussion

7.1 CIZ1 is required for Xi chromosomal movement

Data from this study has confirmed dynamic localisation of the Xi, achieved by transient internalization during S phase. At the time of its replication in primary wild type cells, the Xi moves towards the perinucleolar zone, followed by relocation back to the nuclear periphery after replication. Moreover, CIZ1 plays a crucial role in this relocation event, with genetic deletion of CIZ1 resulting in loss of internalization. This is the first time that CIZ1 has been shown to be involved in chromosomal movement, and to my knowledge the first time a protein has been held accountable for Xi chromatin movement. In addition, culture adaptation resulted in loss of relocation, suggesting that the mechanism of relocation is subject to degeneration upon culture adaptation. Interestingly, additional experiments carried out in the Coverley lab (Stewart et al. 2018) have shown that there is a preferential anchoring of CIZ1, at the Xi, to the nuclear matrix during replication, with over 50% of cells retaining CIZ1 at the Xi after RNase treatment when looking at replicating Xis, compared to 3-7% normally (dependent upon cell line and cycling rate). As Xi movement occurs during replication, anchorage of CIZ1 is occurring during the time at which Xi movement is seen. Therefore, the anchorage of CIZ1 at the Xi to the nuclear matrix may be part of the process that supports Xi movement. This implies that without CIZ1 no anchorage occurs, offering an explanation for the loss of Xi movement in CIZ1 null primary cells. Conversely, no difference was found in terms of CIZ1 anchorage between culture adapted wild type cells and primary wild type cells. Therefore, another unknown event is causing the loss of movement in culture adapted cells.

It is possible that the involvement of CIZ1 in the mechanism of Xi relocation is also applicable to other loci. It has been shown that focal-CIZ1 is present in both male and female nuclei (Ridings-Figueroa et al. 2017) with male and female differentiating embryonic stem cells having similar expression profiles (Sunwoo et al. 2017). Furthermore, a genome-wide effect on polycomb-regulated gene expression is seen following loss of CIZ1 (Stewart et al. 2018). These observations suggest that the behaviour of the Xi could be used as a model to

investigate genome-wide long-range chromatin movement and that CIZ1 likely plays a role in regulation beyond the Xi.

7.2 CIZ1 is required for PRC function at the Xi

Results from my investigation further reinforce the suggestion that CIZ1 is required for routine function of polycomb repressive complexes at the Xi, with gene expression work implying a wider role elsewhere in the genome (Stewart et al. 2018). The unexpected result of chromatin modification re-emergence following culture adaptation in CIZ1 null cells is of interest. The re-emergence alongside the discovery that a shift in EZH2 isoform occurs following culture adaptation (Turner 2017), as well as an increase in protein level of EZH2α, has prompted development of a new hypothesis. This hypothesis was produced while working closely with another student of the Coverley lab, Emma Stewart. Profiling the binding characteristics of EZH2, a subunit of PRC2, revealed that EZH2 is released from spatial constraint upon culture adaptation (Stewart et al. 2018). It is possible that this release occurs as compensation for the loss of chromatin relocation (Chapter 4), enabling the reinstatement of regulatory events, such as H3K27me3 at the Xi, which are crucial for maintenance of the epigenetic state. Based on this proposed hypothesis, an interpretive model was produced (Appendix D; Stewart et al. 2018). The model proposes that there are two alternative pathways by which Xi chromatin and modifying enzymes meet. A CIZ1-dependent relocation pathway in wild type primary cells, where transient relocation allows controlled meeting of Xi chromatin and spatially restricted modifying enzyme, and a CIZ1-independent pathway in culture adapted cells, where elevated ‘free’ enzyme diffuses to the Xi chromatin. The reasoning for the need of two pathways is still unknown. Although completely hypothetical at this point, the movement of chromatin seen in primary cells could signify the need for stringent and efficient targeting of histone modifications, whereas ‘free’ enzyme seen in culture adapted cells could suggest a less rigorous selection of targets. One reason why this may be the case is that primary cells are suggested to be more akin to cells in the body than culture adapted cells. Therefore, stringent target selection is crucial to avoid epigenetic drift that could underpin disease or developmental abnormalities. Conversely, culture adapted cells may sacrifice accuracy for proliferative capability, meaning there could be a larger margin for

error. This increased stability may result in bypassing the need for chromatin movement for chromatin modification. Re-emergence of chromatin modification at the Xi occurred in 23-39% of CIZ1 null culture adapted cells, dependent upon cell line and chromatin modification. It is possible that the threshold for the release of proteins that are responsible for chromatin modifications (for example EZH2) from spatial restraint is different in each cell, resulting in re-emergence occurring in only a proportion of cells. However, this is not understood at this point in time. Investigation via co-staining with EZH2, looking at subnuclear localisation, would provide much needed information. If EZH2 is not colocalising with H3K27me3, EZH2 has not been released, potentially explaining why re-emergence is not seen in all cells.

7.3 Mechanism of Xi relocation

Prior to this study, very little was known regarding the mechanism of Xi relocation. Data presented here are the first steps towards characterising the requirements of Xi chromatin relocation. Analysis via both EdU incorporation and thymidine arrest assays have implicated a number of factors in the relocation process. As summarized in the hypothetical model (Figure 6.8), results have suggested that Xi departure occurs via nuclear myosin-based pathways, requiring DNA polymerase α function, and that Xi return after DNA replication occurs via a combination of (nuclear or cytoplasmic) dynein-based and nuclear myosin-based pathways, possibly acting in a redundant manner. Furthermore, analysis via thymidine arrest produced results that suggest Xi departure is accompanied by an increase in Xi area, which is subsequently reversed after release from arrest. As previously mentioned, the implication of area change is completely speculative, requiring future extensive analysis to reinforce interpretations. Albeit, a change in Xi area has previously been documented. A study found that DNA replication occurs independently of Xi chromosome area, whereas dispersal of the X chromosome is required to allow reactivation after replication (Panova et al. 2013). If this proposition is correct, it is possible that the increase in Xi area seen in my investigation is in response to reactivation. However, since internalisation is dependent on ongoing DNA synthesis, it seems just as likely that the area increase reflects the opening of chromatin to facilitate the entry of replication enzymes. It would be of interest to investigate this, as

understanding the reason for the Xi area change would be an important step towards a complete story. It would also be interesting to visualise Xi relocation in real time via tagged loci and live cell imaging, although this would provide little mechanistic information.

7.4 Further work

There are various avenues that could be taken in order to further develop the results from my work. Primarily, further replicate analyses of thymidine arrest results are required. All inhibitors should be tested in all three wild type cell lines routinely used in this study (E13.1, E13.8 and E14.2). Although results are already significant in most cases, this extended analysis is likely to increase the statistical significance of the results. Achieving a full data set for inhibitory analysis will allow a number of exciting prospects to be discussed, including application of siRNA knockdown to provide more in-depth analysis of the gene-product requirements of Xi relocation. Although time consuming, the use of siRNA to target the genes encoding drivers of Xi relocation, for example nuclear myosin I, would act as concrete evidence supporting results shown here. As relocation failure is observed in CIZ1 null cells, it would be important to test whether the relocation mechanism could be rescued via reintroduction of CIZ1. A line of CIZ1 null primary embryonic fibroblasts that is used in this study (E13.17) was previously manipulated to express full-length GFP-CIZ1 upon induction with doxycycline (Ridings-Figueroa et al. 2017). Therefore, the E13.17 CIZ1 null line can be used to test the effect of CIZ1 reinduction, acting as a direct comparison, adding to the validity of CIZ1's role in relocation as well as promoting CIZ1 as a potential drug target if relocation is recused. Studying CIZ1-protein interactions would also take the story forward. BioID, proximity-dependent biotin identification (Roux et al. 2012), is a new alternative approach which could enable the study of CIZ1-protein interactions. This method could be manipulated to identify proteins in close proximity to CIZ1 at the time of Xi movement. For example, a confirmed interaction between CIZ1 and nuclear myosin I via BioID would further validate the requirement of nuclear myosin I in Xi relocation. The preliminary steps to investigate this using BioID have already begun in the Coverley lab.

7.5 Conclusion

In conclusion, my analysis has confirmed the role of CIZ1 in two important regulatory events, PRC function and Xi relocation, both of which contribute to the maintenance of epigenetic landscape. Crucially, my analysis has also reinforced that culture adapted cell lines do not accurately represent the state of cell found in the body. Notable differences between primary cells and culture adapted cells can be seen throughout. PRC2 subunit isoforms, protein levels, solubility and detrimental loss of chromatin relocation are key prime examples. As mentioned, the nuclear matrix protein CIZ1 and PRCs have been linked with a vast array of diseases including cancers. Therefore, future therapeutic approaches and strategies should be trialled in primary cells to produce results that mimic what would be seen following application in the body, instead of the routine method using cell lines. In addition, my analysis has uncovered the requirements of Xi relocation, producing a valuable hypothetical model interpreting the mechanism. This paves the way for exciting future research that will no doubt aid in the understanding of cancer biology. Furthermore, development of thymidine arrest as a viable assay to study Xi movement will allow a wider breadth of experimental approaches in the near future and has highlighted the importance of taking multiple approaches before coming to a final conclusion.

Appendices

Appendix A

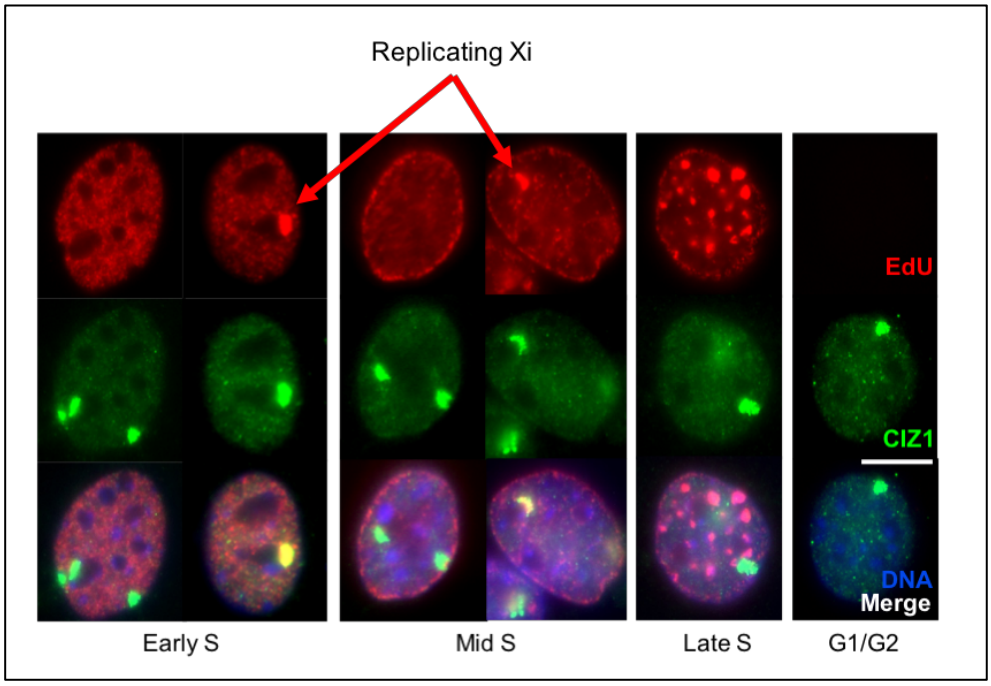

Appendix A. Location and timing of replicating Xi.
Example images of wild type nuclei representing the different stages of the cell cycle, classified as G1/G2 (no label), or early, mid or late S phase based on pattern of EdU incorporation. Immuno-staining for CIZ1 allows determination of replicating Xi and estimation of S phase stage. EdU is red, CIZ1 is green, DNA is blue. Bar is 10 microns. Images taken from Stewart et al. 2018.

Appendix B

Western blot experimental procedure

Gels used for all western blots were Mini-Protean TGX. Gels were aligned into the tank with 500ml glycine/tris/SDS buffer. 5µl of PageRuler^{TM} was loaded as

the ladder; a predefined volume of each sample was loaded to the respective wells. Gels were run at 100V for approximately 60 minutes. Gels were removed and attached to membranes via Invitrogen IBlot machine. Membranes were blocked in 5% milk with 1x PBS and 0.1% Tween 20 or 5% Bovine Serum Albumin (BSA) with 1x TBS (tris buffered saline) and 0.1% Tween 20 for 10 minutes. Membranes were incubated with primary antibodies (Table 2.2) overnight at 4°C. Excess primary antibody was removed via washing with blocking solution three times for 10 minutes each. Membranes were incubated with secondary antibody (Table 2.2) for 60 minutes at room temperature. Excess secondary antibody was removed via washing with wash solution (1x PBS/TBS and 0.1% Tween 20) three times for 15 minutes each. Membranes were exposed to a combination of EZ-ECL solution A and EZ-ECL solution B (Enhanced Chemiluminescence Detection Kit for HRP) and were visualised using PXi.

Appendix C

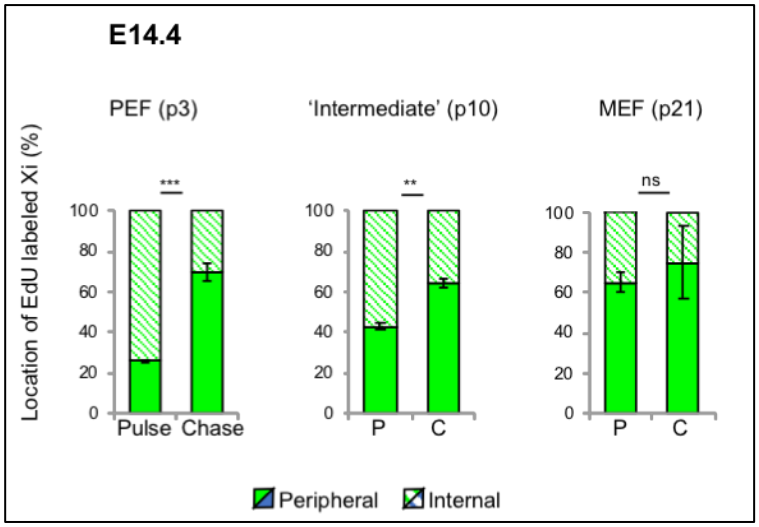

Appendix C. Location of CIZ1-marked and EdU-labelled Xi in E14.4 wild type fibroblasts.

Gradual loss of relocation is seen as passage number increases, passage number is shown in brackets. Data for E14.4 p10 was generated by Victoria Scott.

Appendix D

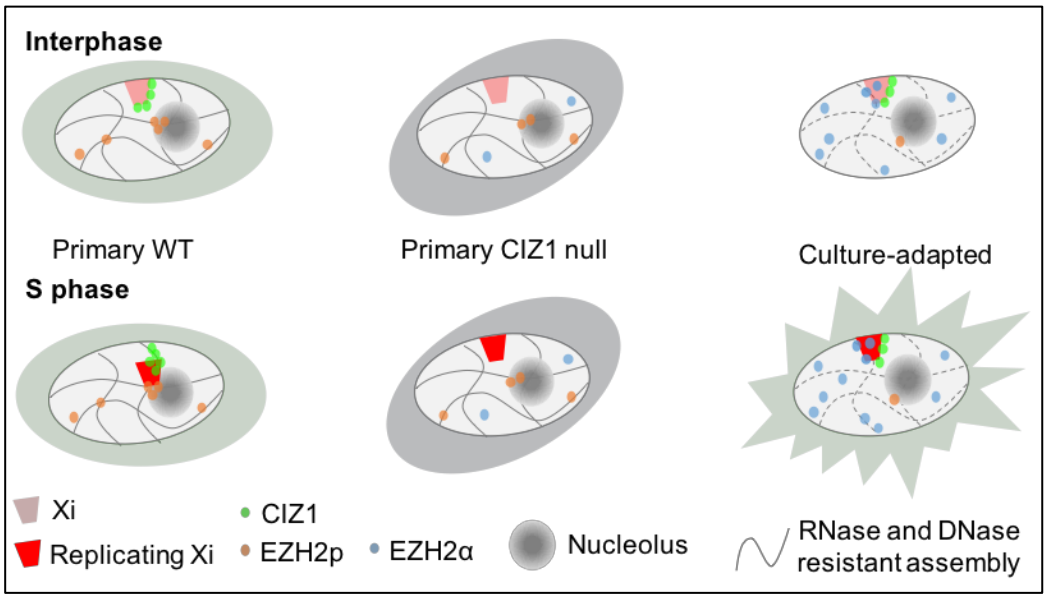

Appendix D. Summary model depicting two alternative pathways by which chromatin and modifying enzymes could meet.

A CIZ1-dependent Xi relocation pathway, with anchored and spatially restricted EZH2p (orange) in wild type primary cells (left). Compromised Xi relocation and loss of marks from the Xi in CIZ1 null primary cells (centre). A CIZ1-independent pathway, with elevated “free” EZH2α (blue) diffusing to the Xi (right). Model taken from Stewart et al. 2018.

References; in the style of Cell Journal

Ainscough, J.F.-X., Rahman, F.A., Sercombe, H., Sedo, A., Gerlach, B., and Coverley, D. (2007). C-terminal domains deliver the DNA replication factor Ciz1 to the nuclear matrix. J. Cell Sci. *120*, 115–124.

Almeida, M., Pintacuda, G., Masui, O., Koseki, Y., Gdula, M., Cerase, A., Brown, D., Mould, A., Innocent, C., Nakayama, M., et al. (2017). PCGF3/5-PRC1 initiates Polycomb recruitment in X chromosome inactivation. Science *356*, 1081–1084.

Anachkova, B., Djeliova, V., and Russev, G. (2005). Nuclear matrix support of DNA replication. J. Cell. Biochem. *96*, 951–961.

Augui, S., Nora, E.P., and Heard, E. (2011). Regulation of X-chromosome inactivation by the X-inactivation centre. Nat. Rev. Genet. *12*, 429–442.

Barakat, T.S., Loos, F., van Staveren, S., Myronova, E., Ghazvini, M., Grootegoed, J.A., and Gribnau, J. (2014). The trans-activator RNF12 and cis-acting elements effectuate X chromosome inactivation independent of X-pairing. Mol. Cell *53*, 965–978.

Baranovskiy, A.G., Babayeva, N.D., Suwa, Y., Gu, J., Pavlov, Y.I., and Tahirov, T.H. (2014). Structural basis for inhibition of DNA replication by aphidicolin. Nucleic Acids Res. *42*, 14013–14021.

Barr, M.L., and Bertram, E.G. (1949). A morphological distinction between neurones of the male and female, and the behaviour of the nucleolar satellite during accelerated nucleoprotein synthesis. Nature *163*, 676.

Baylin, S.B., and Jones, P.A. (2011). A decade of exploring the cancer epigenome — biological and translational implications. Nat. Rev. Cancer *11*, 726.

Berezney, R., and Coffey, D.S. (1974). Identification of a nuclear protein matrix. Biochem. Biophys. Res. Commun. *60*, 1410–1417.

Bodnar, A.G., Ouellette, M., Frolkis, M., Holt, S.E., Chiu, C.P., Morin, G.B., Harley, C.B., Shay, J.W., Lichtsteiner, S., and Wright, W.E. (1998). Extension of life-span by introduction of telomerase into normal human cells. Science *279*, 349–352.

Borensztein, M., Syx, L., Ancelin, K., Diabangouaya, P., Picard, C., Liu, T., Liang, J.-B., Vassilev, I., Galupa, R., Servant, N., et al. (2017). Xist-dependent imprinted X inactivation and the early developmental consequences of its failure. Nat. Struct. Mol. Biol. *24*, 226–233.

Brown, C.J., Hendrich, B.D., Rupert, J.L., Lafrenière, R.G., Xing, Y., Lawrence, J., and Willard, H.F. (1992). The human XIST gene: analysis of a 17 kb inactive X-specific RNA that contains conserved repeats and is highly localized within the nucleus. Cell *71*, 527–542.

Cao, R., Wang, L., Wang, H., Xia, L., Erdjument-Bromage, H., Tempst, P., Jones, R.S., and Zhang, Y. (2002). Role of histone H3 lysine 27 methylation in Polycomb-group silencing. Science *298*, 1039–1043.

Casas-Delucchi, C.S., Brero, A., Rahn, H.-P., Solovei, I., Wutz, A., Cremer, T., Leonhardt, H., and Cardoso, M.C. (2011). Histone acetylation controls the inactive X chromosome replication dynamics. Nat. Commun. *2*, 222.

Chen, C.-K., Blanco, M., Jackson, C., Aznauryan, E., Ollikainen, N., Surka, C., Chow, A., Cerase, A., McDonel, P., and Guttman, M. (2016). Xist recruits the X chromosome to the nuclear lamina to enable chromosome-wide silencing. Science *354*, 468–472.

Chuang, C.-H., Carpenter, A.E., Fuchsova, B., Johnson, T., de Lanerolle, P., and Belmont, A.S. (2006). Long-range directional movement of an interphase chromosome site. Curr. Biol. *16*, 825–831.

Chubb, J.R., Boyle, S., Perry, P., and Bickmore, W.A. (2002). Chromatin motion is constrained by association with nuclear compartments in human cells. Curr.

Biol. *12*, 439–445.

Copeland, N.A., Sercombe, H.E., Ainscough, J.F.X., and Coverley, D. (2010). Ciz1 cooperates with cyclin-A-CDK2 to activate mammalian DNA replication in vitro. J. Cell Sci. *123*, 1108–1115.

Copeland, N.A., Sercombe, H.E., Wilson, R.H.C., and Coverley, D. (2015). Cyclin-A-CDK2-mediated phosphorylation of CIZ1 blocks replisome formation and initiation of mammalian DNA replication. J. Cell Sci. *128*, 1518–1527.

Coverley, D., Marr, J., and Ainscough, J. (2005). Ciz1 promotes mammalian DNA replication. J. Cell Sci. *118*, 101–112.

Dahmcke, C.M., Büchmann-Møller, S., Jensen, N.A., and Mitchelmore, C. (2008). Altered splicing in exon 8 of the DNA replication factor CIZ1 affects subnuclear distribution and is associated with Alzheimer's disease. Mol. Cell. Neurosci. *38*, 589–594.

Fang, J., Chen, T., Chadwick, B., Li, E., and Zhang, Y. (2004). Ring1b-mediated H2A ubiquitination associates with inactive X chromosomes and is involved in initiation of X inactivation. J. Biol. Chem. *279*, 52812–52815.

Firestone, A.J., Weinger, J.S., Maldonado, M., Barlan, K., Langston, L.D., O'Donnell, M., Gelfand, V.I., Kapoor, T.M., and Chen, J.K. (2012). Small-molecule inhibitors of the AAA+ ATPase motor cytoplasmic dynein. Nature *484*, 125–129.

Fried, J., Perez, A.G., Doblin, J.M., and Clarkson, B.D. (1981). Cytotoxic and cytokinetic effects of thymidine, 5-fluorouracil, and deoxycytidine on HeLa cells in culture. Cancer Res. *41*, 2627–2632.

Galupa, R., and Heard, E. (2015). X-chromosome inactivation: new insights into cis and trans regulation. Curr. Opin. Genet. Dev. *31*, 57–66.

Gribnau, J., and Grootegoed, J.A. (2012). Origin and evolution of X chromosome

inactivation. Curr. Opin. Cell Biol. *24*, 397–404.

Harley, C.B., Futcher, A.B., and Greider, C.W. (1990). Telomeres shorten during ageing of human fibroblasts. Nature *345*, 458–460.

Hasegawa, Y., Brockdorff, N., Kawano, S., Tsutui, K., Tsutui, K., and Nakagawa, S. (2010). The matrix protein hnRNP U is required for chromosomal localization of Xist RNA. Dev. Cell *19*, 469–476.

Hayflick, L., and Moorhead, P.S. (1961). The serial cultivation of human diploid cell strains. Exp. Cell Res. *25*, 585–621.

Higgins, G., Roper, K.M., Watson, I.J., Blackhall, F.H., Rom, W.N., Pass, H.I., Ainscough, J.F.X., and Coverley, D. (2012). Variant Ciz1 is a circulating biomarker for early-stage lung cancer. Proc. Natl. Acad. Sci. U. S. A. *109*, E3128–E3135.

den Hollander, P., and Kumar, R. (2006). Dynein light chain 1 contributes to cell cycle progression by increasing cyclin-dependent kinase 2 activity in estrogen-stimulated cells. Cancer Res. *66*, 5941–5949.

den Hollander, P., Rayala, S.K., Coverley, D., and Kumar, R. (2006). Ciz1, a Novel DNA-binding coactivator of the estrogen receptor alpha, confers hypersensitivity to estrogen action. Cancer Res. *66*, 11021–11029.

Jonkers, I., Barakat, T.S., Achame, E.M., Monkhorst, K., Kenter, A., Rentmeester, E., Grosveld, F., Grootegoed, J.A., and Gribnau, J. (2009). RNF12 is an X-Encoded dose-dependent activator of X chromosome inactivation. Cell *139*, 999–1011.

Kim, H., Kang, K., and Kim, J. (2009). AEBP2 as a potential targeting protein for Polycomb Repression Complex PRC2. Nucleic Acids Res. *37*, 2940–2950.

Kim, N.-S., Hahn, Y., Oh, J.-H., Lee, J.-Y., Oh, K.-J., Kim, J.-M., Park, H.-S., Kim, S., Song, K.-S., Rho, S.-M., et al. (2004). Gene cataloging and expression

profiling in human gastric cancer cells by expressed sequence tags. Genomics *83*, 1024–1045.

Koehler, D.R., and Hanawalt, P.C. (1996). Recruitment of damaged DNA to the nuclear matrix in hamster cells following ultraviolet irradiation. Nucleic Acids Res. *24*, 2877–2884.

Kulashreshtha, M., Mehta, I.S., Kumar, P., and Rao, B.J. (2016). Chromosome territory relocation during DNA repair requires nuclear myosin 1 recruitment to chromatin mediated by Y-H2AX signaling. Nucleic Acids Res. *44*, 8272–8291.

Kuzmichev, A., Nishioka, K., Erdjument-Bromage, H., Tempst, P., and Reinberg, D. (2002). Histone methyltransferase activity associated with a human multiprotein complex containing the Enhancer of Zeste protein. Genes Dev. *16*, 2893–2905.

Lee, J.T., Davidow, L.S., and Warshawsky, D. (1999). Tsix, a gene antisense to Xist at the X-inactivation centre. Nat. Genet. *21*, 400–404.

Levine, S.S., Weiss, A., Erdjument-Bromage, H., Shao, Z., Tempst, P., and Kingston, R.E. (2002). The core of the polycomb repressive complex is compositionally and functionally conserved in flies and humans. Mol. Cell. Biol. *22*, 6070–6078.

Lippert, L.G., Dadosh, T., Diroll, B.T., Hallock, J.T., Murray, C.B., Holzbaur, E.L.F., Reck-Peterson, S.L., and Goldman, Y.E. (2015). Cytoplasmic Dynein Ring Tilting Detected by Combined polTIRF and Sub-Pixel Particle Tracking of Semiconductor Quantum Rods. Biophys. J. *108*, 22a.

Liu, T., Ren, X., Li, L., Yin, L., Liang, K., Yu, H., Ren, H., Zhou, W., Jing, H., and Kong, C. (2015). Ciz1 promotes tumorigenicity of prostate carcinoma cells. Front. Biosci. *20*, 705–715.

Lundblad, V., and Szostak, J.W. (1989). A mutant with a defect in telomere elongation leads to senescence in yeast. Cell *57*, 633–643.

Lyon, M.F. (1961). Gene action in the X-chromosome of the mouse (Mus musculus L.). Nature *190*, 372–373.

Lyu, G., Tan, T., Guan, Y., Sun, L., Liang, Q., and Tao, W. (2018). Changes in the position and volume of inactive X chromosomes during the G0/G1 transition. Chromosome Res. *26*, 179–189.

Ma, H.T., and Poon, R.Y.C. (2011). Synchronization of HeLa cells. Methods Mol. Biol. *761*, 151–161.

Margueron, R., and Reinberg, D. (2011). The Polycomb complex PRC2 and its mark in life. Nature *469*, 343–349.

Mehta, I.S., Amira, M., Harvey, A.J., and Bridger, J.M. (2010). Rapid chromosome territory relocation by nuclear motor activity in response to serum removal in primary human fibroblasts. Genome Biol. *11*, R5.

Mitsui, K., Matsumoto, A., Ohtsuka, S., Ohtsubo, M., and Yoshimura, A. (1999). Cloning and characterization of a novel p21(Cip1/Waf1)-interacting zinc finger protein, ciz1. Biochem. Biophys. Res. Commun. *264*, 457–464.

Mohammad, F., Pandey, R.R., Nagano, T., Chakalova, L., Mondal, T., Fraser, P., and Kanduri, C. (2008). Kcnq1ot1/Lit1 noncoding RNA mediates transcriptional silencing by targeting to the perinucleolar region. Mol. Cell. Biol. *28*, 3713–3728.

Morris, N.R., Reichard, P., and Fischer, G.A. (1963). Studies concerning the inhibition of cellular reproduction by deoxyribonucleosides: II. Inhibition of the synthesis of deoxycytidine by thymidine, deoxyadenosine and deoxyguanosine. Biochimica et Biophysica Acta (BBA) - Specialized Section on Nucleic Acids and Related Subjects *68*, 93–99.

Muyrers-Chen, I., Hernández-Muñoz, I., Lund, A.H., Valk-Lingbeek, M.E., van der Stoop, P., Boutsma, E., Tolhuis, B., Bruggeman, S.W.M., Taghavi, P., Verhoeven, E., et al. (2004). Emerging roles of Polycomb silencing in X-

inactivation and stem cell maintenance. Cold Spring Harb. Symp. Quant. Biol. *69*, 319–326.

de Napoles, M., Mermoud, J.E., Wakao, R., Tang, Y.A., Endoh, M., Appanah, R., Nesterova, T.B., Silva, J., Otte, A.P., Vidal, M., et al. (2004). Polycomb group proteins Ring1A/B link ubiquitylation of histone H2A to heritable gene silencing and X inactivation. Dev. Cell *7*, 663–676.

Navarro, P., Chambers, I., Karwacki-Neisius, V., Chureau, C., Morey, C., Rougeulle, C., and Avner, P. (2008). Molecular coupling of Xist regulation and pluripotency. Science *321*, 1693–1695.

Otsu, N. (1979). A Threshold Selection Method from Gray-Level Histograms. IEEE Trans. Syst. Man Cybern. *9*, 62–66.

Pandey, R.R., Mondal, T., Mohammad, F., Enroth, S., Redrup, L., Komorowski, J., Nagano, T., Mancini-Dinardo, D., and Kanduri, C. (2008). Kcnq1ot1 antisense noncoding RNA mediates lineage-specific transcriptional silencing through chromatin-level regulation. Mol. Cell *32*, 232–246.

Panova, A.V., Nekrasov, E.D., Lagarkova, M.A., Kiselev, S.L., and Bogomazova, A.N. (2013). Late replication of the inactive x chromosome is independent of the compactness of chromosome territory in human pluripotent stem cells. Acta Naturae *5*, 54–61.

Paschal, B.M., and Vallee, R.B. (1987). Retrograde transport by the microtubule-associated protein MAP 1C. Nature *330*, 181–183.

Pestic-Dragovich, L., Stojiljkovic, L., Philimonenko, A.A., Nowak, G., Ke, Y., Settlage, R.E., Shabanowitz, J., Hunt, D.F., Hozak, P., and de Lanerolle, P. (2000). A myosin I isoform in the nucleus. Science *290*, 337–341.

Pintacuda, G., Wei, G., Roustan, C., Kirmizitas, B.A., Solcan, N., Cerase, A., Castello, A., Mohammed, S., Moindrot, B., Nesterova, T.B., et al. (2017). hnRNPK Recruits PCGF3/5-PRC1 to the Xist RNA B-Repeat to Establish

Polycomb-Mediated Chromosomal Silencing. Mol. Cell *68*, 955–969.e10.

Raaphorst, F.M. (2005). Deregulated expression of Polycomb-group oncogenes in human malignant lymphomas and epithelial tumors. Hum. Mol. Genet. *14 Spec No 1*, R93–R100.

Rahman, F.A., Ainscough, J.F.-X., Copeland, N., and Coverley, D. (2007). Cancer-associated missplicing of exon 4 influences the subnuclear distribution of the DNA replication factor CIZ1. Hum. Mutat. *28*, 993–1004.

Rahman, F.A., Aziz, N., and Coverley, D. (2010). Differential detection of alternatively spliced variants of Ciz1 in normal and cancer cells using a custom exon-junction microarray. BMC Cancer *10*, 482.

Ridings-Figueroa, R., Stewart, E.R., Nesterova, T.B., Coker, H., Pintacuda, G., Godwin, J., Wilson, R., Haslam, A., Lilley, F., Ruigrok, R., et al. (2017). The nuclear matrix protein CIZ1 facilitates localization of Xist RNA to the inactive X-chromosome territory. Genes Dev. *31*, 876–888.

Robinson, S.I., Small, D., Idzerda, R., McKnight, G.S., and Vogelstein, B. (1983). The association of transcriptionally active genes with the nuclear matrix of the chicken oviduct. Nucleic Acids Res. *11*, 5113–5130.

da Rocha, S.T., Boeva, V., Escamilla-Del-Arenal, M., Ancelin, K., Granier, C., Matias, N.R., Sanulli, S., Chow, J., Schulz, E., Picard, C., et al. (2014). Jarid2 Is Implicated in the Initial Xist-Induced Targeting of PRC2 to the Inactive X Chromosome. Mol. Cell *53*, 301–316.

Roux, K.J., Kim, D.I., Raida, M., and Burke, B. (2012). A promiscuous biotin ligase fusion protein identifies proximal and interacting proteins in mammalian cells. J. Cell Biol. *196*, 801–810.

Sado, T., and Brockdorff, N. (2013). Advances in understanding chromosome silencing by the long non-coding RNA Xist. Philos. Trans. R. Soc. Lond. B Biol. Sci. *368*, 20110325.

Sarma, K., Cifuentes-Rojas, C., Ergun, A., Del Rosario, A., Jeon, Y., White, F., Sadreyev, R., and Lee, J.T. (2014). ATRX directs binding of PRC2 to Xist RNA and Polycomb targets. Cell *159*, 869–883.

Sato, T., Kaneda, A., Tsuji, S., Isagawa, T., Yamamoto, S., Fujita, T., Yamanaka, R., Tanaka, Y., Nukiwa, T., Marquez, V.E., et al. (2013). PRC2 overexpression and PRC2-target gene repression relating to poorer prognosis in small cell lung cancer. Sci. Rep. *3*, 1911.

Schindelin, J., Arganda-Carreras, I., Frise, E., Kaynig, V., Longair, M., Pietzsch, T., Preibisch, S., Rueden, C., Saalfeld, S., Schmid, B., et al. (2012). Fiji: an open-source platform for biological-image analysis. Nat. Methods *9*, 676–682.

Schroer, T.A., Steuer, E.R., and Sheetz, M.P. (1989). Cytoplasmic dynein is a minus end-directed motor for membranous organelles. Cell *56*, 937–946.

Schwartz, Y.B., and Pirrotta, V. (2007). Polycomb silencing mechanisms and the management of genomic programmes. Nat. Rev. Genet. *8*, 9–22.

Schwartz, Y.B., and Pirrotta, V. (2013). A new world of Polycombs: unexpected partnerships and emerging functions. Nat. Rev. Genet. *14*, 853–864.

Shay, J.W., Pereira-Smith, O.M., and Wright, W.E. (1991). A role for both RB and p53 in the regulation of human cellular senescence. Exp. Cell Res. *196*, 33–39.

Sirchia, S.M., Ramoscelli, L., Grati, F.R., Barbera, F., Coradini, D., Rossella, F., Porta, G., Lesma, E., Ruggeri, A., Radice, P., et al. (2005). Loss of the inactive X chromosome and replication of the active X in BRCA1-defective and wild-type breast cancer cells. Cancer Res. *65*, 2139–2146.

Stewart, E., Turner, R., et al. (2018). Maintenance of epigenetic landscape requires CIZ1 and is corrupted in differentiated fibroblasts in long-term culture. To be published in Nat. Commun. [Paper #NCOMMS-18-15349B].

Sunwoo, H., Colognori, D., Froberg, J.E., Jeon, Y., and Lee, J.T. (2017). Repeat E anchors Xist RNA to the inactive X chromosomal compartment through CDKN1A-interacting protein (CIZ1). Proc. Natl. Acad. Sci. U. S. A. *114*, 10654–10659.

Turner, R. (2017). Analysis of Polycomb Repressive Complex 2 expression in CIZ1 Null mice. BSc Hons dissertation, University of York, York.

Valk-Lingbeek, M.E., Bruggeman, S.W.M., and van Lohuizen, M. (2004). Stem cells and cancer; the polycomb connection. Cell *118*, 409–418.

Wang, D.-Q., Wang, K., Yan, D.-W., Liu, J., Wang, B., Li, M.-X., Wang, X.-W., Liu, J., Peng, Z.-H., Li, G.-X., et al. (2014). Ciz1 is a novel predictor of survival in human colon cancer. Exp. Biol. Med. *239*, 862–870.

Wang, H., Wang, L., Erdjument-Bromage, H., Vidal, M., Tempst, P., Jones, R.S., and Zhang, Y. (2004). Role of histone H2A ubiquitination in Polycomb silencing. Nature *431*, 873–878.

Watson, J.D. (1972). Origin of concatemeric T7 DNA. Nat. New Biol. *239*, 197–201.

Wiles, E.T., and Selker, E.U. (2017). H3K27 methylation: a promiscuous repressive chromatin mark. Curr. Opin. Genet. Dev. *43*, 31–37.

Wu, J., Lei, L., Gu, D., Liu, H., and Wang, S. (2016). CIZ1 is upregulated in hepatocellular carcinoma and promotes the growth and migration of the cancer cells. Tumour Biol. *37*, 4735–4742.

Xiao, J., Uitti, R.J., Zhao, Y., Vemula, S.R., Perlmutter, J.S., Wszolek, Z.K., Maraganore, D.M., Auburger, G., Leube, B., Lehnhoff, K., et al. (2012). Mutations in CIZ1 cause adult onset primary cervical dystonia. Ann. Neurol. *71*, 458–469.

Yang, F., Deng, X., Ma, W., Berletch, J.B., Rabaia, N., Wei, G., Moore, J.M., Filippova, G.N., Xu, J., Liu, Y., et al. (2015). The lncRNA Firre anchors the

inactive X chromosome to the nucleolus by binding CTCF and maintains H3K27me3 methylation. Genome Biol. *16*, 52.

Yildirim, E., Kirby, J.E., Brown, D.E., Mercier, F.E., Sadreyev, R.I., Scadden, D.T., and Lee, J.T. (2013). Xist RNA is a potent suppressor of hematologic cancer in mice. Cell *152*, 727–742.

Yoo, K.H., and Hennighausen, L. (2012). EZH2 methyltransferase and H3K27 methylation in breast cancer. Int. J. Biol. Sci. *8*, 59–65.

Zeitlin, S., Parent, A., Silverstein, S., and Efstratiadis, A. (1987). Pre-mRNA splicing and the nuclear matrix. Mol. Cell. Biol. *7*, 111–120.

Zhang, D., Wang, Y., Dai, Y., Wang, J., Suo, T., Pan, H., Liu, H., Shen, S., and Liu, H. (2015). CIZ1 promoted the growth and migration of gallbladder cancer cells. Tumour Biol. *36*, 2583–2591.

Zhang, L.-F., Huynh, K.D., and Lee, J.T. (2007). Perinucleolar targeting of the inactive X during S phase: evidence for a role in the maintenance of silencing. Cell *129*, 693–706.